STOCHASTIC GREY-BOX MODELLING AS A TOOL FOR IMPROVING THE QUALITY OF FIRST ENGINEERING PRINCIPLES MODELS

Niels Rode Kristensen [*,1] **Henrik Madsen** [**]
Sten Bay Jørgensen [*]

[*] *Department of Chemical Engineering, Technical University of Denmark, Building 229, DK-2800 Lyngby, Denmark*
[**] *Informatics and Mathematical Modelling, Technical University of Denmark, Building 321, DK-2800 Lyngby, Denmark*

Abstract: A systematic framework for improving the quality of first engineering principles models using experimental data is presented. The framework is based on stochastic grey-box modelling and incorporates statistical tests and nonparametric regression in a manner that permits systematic iterative model improvement. More specifically, the proposed framework provides features that allow model deficiencies to be pinpointed and their structural origin to be uncovered through estimation of unknown functional relations. The performance of the proposed framework is illustrated through a case study involving a model of a fed-batch bioreactor, where it is shown how an incorrectly modelled biomass growth rate can be uncovered and a more appropriate functional relation inferred.

Keywords: Stochastic modelling, parameter estimation, statistical inference, nonparametric regression, iterative improvement.

1. INTRODUCTION

Dynamic model development is an inherently purpose-driven act in the sense that the required accuracy of a model depends on its intended application, and developing a suitable model for a given purpose involves a fundamental trade-off between model accuracy and model simplicity (Raisch, 2000). For models intended for simulation and optimisation purposes, which must be valid over wide ranges of state space, the required model accuracy and hence the necessary model complexity is high, which means that developing such models is potentially time-consuming.

Ordinary differential equation (ODE) models developed from first engineering principles and physical insights are typically used for such purposes and a common problem with the development of such models is that only the basic structure of the model can be determined directly from first engineering principles, whereas a number of constitutive equations describing e.g. reaction kinetics often remain to be determined from experimental data, which may be difficult. Furthermore, if the quality of a model of this type proves to be too low, few systematic methods are available for determining how to improve the model. Altogether, this often renders the development of first engineering principles models very time-consuming.

[1] Corresponding author.

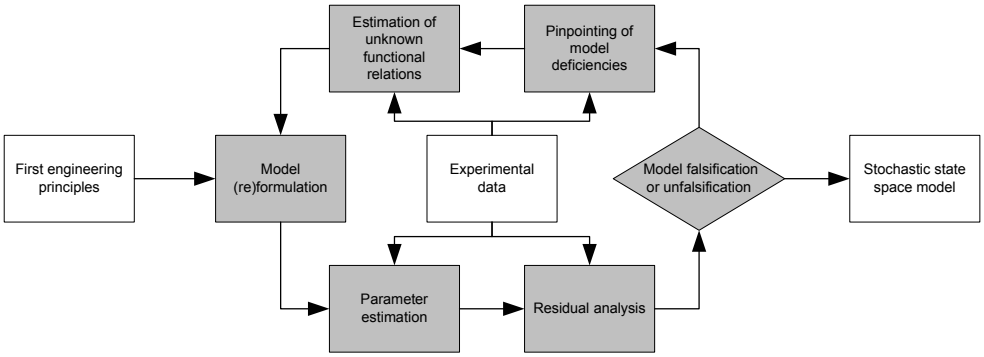

Fig. 1. The proposed grey-box modelling cycle. The boxes in grey illustrate tasks and the boxes in white illustrate inputs to and outputs from the modelling cycle.

In the present paper stochastic grey-box modelling is proposed as a tool for systematic improvement of first engineering principles models, as this approach resolves some of the issues mentioned above. In particular, the proposed framework facilitates pinpointing of model deficiencies and provides means to subsequently uncover the structural origin of these deficiencies through estimation of unknown functional relations. To obtain these estimates nonparametric modelling is applied, and the integration of nonparametric modelling with conventional stochastic grey-box modelling into a systematic framework for improving the quality of first engineering principles models is the key new contribution of the paper.

The remainder of the paper is organized as follows: In Section 2 the proposed framework is outlined and in Section 3 a case study demonstrating its performance is given. Finally, in Section 4, the conclusions of the paper are presented.

2. METHODOLOGY

A diagram of the proposed framework is shown in Figure 1 in the form of a modelling cycle, which shows the individual steps of the corresponding iterative model development procedure. These steps are explained in more detail in the following.

2.1 Model (re)formulation

A basic assumption of the proposed framework is that an initial ODE model, derived from first engineering principles, is available, which needs to be improved to serve its intended purpose. The first step of the modelling cycle then deals with model (re)formulation, which essentially means translation of the ODE model into a stochastic grey-box model (or modification of this model in subsequent modelling cycle iterations).

Stochastic grey-box models are state space models consisting of a set of stochastic differential equations (SDE's) describing the dynamics of the system in continuous time and a set of discrete time measurement equations, i.e.:

$$d\boldsymbol{x}_t = \boldsymbol{f}(\boldsymbol{x}_t, \boldsymbol{u}_t, t, \boldsymbol{\theta})dt + \boldsymbol{\sigma}(\boldsymbol{u}_t, t, \boldsymbol{\theta})d\boldsymbol{\omega}_t \quad (1)$$

$$\boldsymbol{y}_k = \boldsymbol{h}(\boldsymbol{x}_k, \boldsymbol{u}_k, t_k, \boldsymbol{\theta}) + \boldsymbol{e}_k \quad (2)$$

where $t \in \mathbb{R}$ is time, $\boldsymbol{x}_t \in \mathbb{R}^n$ is a vector of state variables, $\boldsymbol{u}_t \in \mathbb{R}^m$ is a vector of input variables, $\boldsymbol{y}_k \in \mathbb{R}^l$ is a vector of measured output variables, $\boldsymbol{\theta} \in \mathbb{R}^p$ is a vector of parameters, $\boldsymbol{f}(\cdot) \in \mathbb{R}^n$, $\boldsymbol{\sigma}(\cdot) \in \mathbb{R}^{n \times n}$ and $\boldsymbol{h}(\cdot) \in \mathbb{R}^l$ are nonlinear functions, $\{\boldsymbol{\omega}_t\}$ is an n-dimensional standard Wiener process and $\{\boldsymbol{e}_k\}$ is an l-dimensional white noise process with $\boldsymbol{e}_k \in N(\boldsymbol{0}, \boldsymbol{S}(\boldsymbol{u}_k, t_k, \boldsymbol{\theta}))$.

A considerable advantage of models of this type is that they are designed to accommodate random effects due to e.g. approximation errors or unmodelled phenomena through the diffusion term of the SDE's in (1), which means that estimation of the parameters of this term from experimental data provides a measure of model uncertainty. This is a key point and forms the basis of the proposed framework for systematic model improvement.

2.2 Parameter estimation

In the second step of the modelling cycle the idea therefore is to estimate the unknown parameters of the model in (1)-(2) from experimental data, including the parameters of the diffusion term.

Stochastic grey-box models allow for a decomposition of the noise affecting the system into a process noise term (the diffusion term) and a measurement noise term. As a result unknown parameters of such models can be estimated from experimental data in a *prediction error* (PE) setting, whereas for standard ODE models it can only be done in an *output error* (OE) setting, which tends to give biased and less reproducable results, because random effects are absorbed into

the parameter estimates (Young, 1981). Furthermore, since the solution to (1) is a Markov process, an estimation scheme based on probabilistic methods can be applied, e.g. *maximum likelihood* (ML) or *maximum a posteriori* (MAP). An efficient such scheme, based on the extended Kalman filter (EKF), is available (Kristensen *et al.*, 2002*b*).

2.3 Residual analysis

In the third step of the modelling cycle the idea is to evaluate the quality of the model once the unknown parameters have been estimated. The most important aspect in this regard is to investigate the predictive capabilities of the model by performing cross-validation residual analysis, and various methods are available for this purpose.

2.4 Model falsification or unfalsification

The fourth step of the modelling cycle is the important step of *model falsification or unfalsification*, which deals with whether or not, based on the information obtained in the previous step, the model is sufficiently accurate to serve its intended purpose. In practice, this is a subjective decision, as it involves addressing the trade-off between necessary model accuracy and affordable model complexity with respect to the specific intended purpose of the model. If, based on this decision, the model is unfalsified, the model development procedure can be terminated, but if the model is falsified, the modelling cycle must be repeated by re-formulating the model. In the latter case, the properties of the model in (1)-(2) facilitate the task at hand as shown in the following.

2.5 Pinpointing of model deficiencies

In the fifth step of the modelling cycle, which is only needed if the model has been falsified, the idea is to apply statistical tests to provide indications of which parts of the model that are deficient. The key statistical tests needed for this purpose are tests for significance of the individual parameters, particularly the parameters of the diffusion term, and as it turns out, the properties of the ML and MAP estimators mentioned above allow t-tests to be applied for this purpose.

These tests provide the necessary framework for obtaining indications of which parts of the model that are deficient. In principle, *insignificant* parameters are parameters that may be eliminated, and the presence of such parameters is therefore an indication that the model is overparameterized. On the other hand, because of the particular nature of the model in (1)-(2), where the diffusion term is included to account for random effects due to e.g. approximation errors or unmodelled phenomena, the presence of *significant* parameters in the diffusion term is an indication that the corresponding drift term is incorrect, which in turn provides an uncertainty measure that allows model deficiencies to be detected. If, instead of the general parameterization of the diffusion term indicated in (1), a diagonal parameterization is used, this also allows the deficiencies to be pinpointed in the sense that deficiencies in specific elements of the drift term can be detected, which in turn provides an error indicator for the constitutive equations or phenomena models influencing this term. If, by using physical insights, it is subsequently possible to select a specific phenomena model for further investigation, the proposed framework also provides means to confirm if the suspicion that this model is incorrect is true.

Typical suspect phenomena models include models of reaction rates, heat and mass transfer rates and similar complex dynamic phenomena, all of which can usually be described using functions of the state and input variables, i.e.:

$$r_t = \varphi(\boldsymbol{x}_t, \boldsymbol{u}_t, \boldsymbol{\theta}) \tag{3}$$

where r_t is a phenomenon of interest and $\varphi(\cdot) \in \mathbb{R}$ is the nonlinear function used to describe it. To confirm if the suspicion that $\varphi(\cdot)$ is incorrect is true, the parameter estimation step must be repeated with a re-formulated version of the model in (1)-(2), where r_t is isolated by including it as an additional state variable, i.e.:

$$d\boldsymbol{x}_t^* = \boldsymbol{f}^*(\boldsymbol{x}_t^*, \boldsymbol{u}_t, t, \boldsymbol{\theta})dt + \boldsymbol{\sigma}^*(\boldsymbol{u}_t, t, \boldsymbol{\theta})d\boldsymbol{\omega}_t^* \tag{4}$$

$$\boldsymbol{y}_k = \boldsymbol{h}(\boldsymbol{x}_k^*, \boldsymbol{u}_k, t_k, \boldsymbol{\theta}) + \boldsymbol{e}_k \tag{5}$$

where $\boldsymbol{x}_t^* = [\boldsymbol{x}_t^T \; r_t]^T$ is the extended state vector, $\boldsymbol{\sigma}^*(\cdot) \in \mathbb{R}^{(n+1)\times(n+1)}$ is the extended diffusion term and $\{\boldsymbol{\omega}_t^*\}$ is an $(n+1)$-dimensional standard Wiener process. The extended drift term can be derived from the original drift term as follows:

$$\boldsymbol{f}^*(\boldsymbol{x}_t^*, \boldsymbol{u}_t, t, \boldsymbol{\theta}) = \begin{pmatrix} \boldsymbol{f}(\boldsymbol{x}_t, \boldsymbol{u}_t, t, \boldsymbol{\theta}) \\ \dfrac{\partial \varphi(\boldsymbol{x}_t, \boldsymbol{u}_t, \boldsymbol{\theta})}{\partial \boldsymbol{x}_t}\dfrac{d\boldsymbol{x}_t}{dt} + \dfrac{\partial \varphi(\boldsymbol{x}_t, \boldsymbol{u}_t, \boldsymbol{\theta})}{\partial \boldsymbol{u}_t}\dfrac{d\boldsymbol{u}_t}{dt} \end{pmatrix} \tag{6}$$

The presence of significant parameters in the corresponding diagonal element of the extended diffusion term is then an indication that $\varphi(\cdot)$ is incorrect and in turn confirms the suspicion.

2.6 Estimation of unknown functional relations

In the sixth step of the modelling cycle, which can only be used if specific model deficiencies have been pinpointed as described above, the idea is to uncover the structural origin of these deficiencies.

The corresponding procedure is based on a combination of the applicability of stochastic grey-box models for state estimation and the ability of nonparametric regression methods to provide visualizable estimates of unknown functional relations with associated confidence intervals.

Using the re-formulated model in (4)-(5) and the corresponding parameter estimates, state estimates $\hat{\boldsymbol{x}}^*_{k|k}$, $k = 0, \ldots, N$, can be obtained for a given set of experimental data by applying the EKF. In particular, since the incorrectly modelled phenomenon r_t is included as an additional state variable in this model, estimates $\hat{r}_{k|k}$, $k = 0, \ldots, N$, can be obtained, which in turn facilitates application of nonparametric regression to provide estimates of possible functional relations between r_t and the state and input variables.

Several nonparametric regression techniques are available (Hastie *et al.*, 2001), but in the context of the proposed framework, *additive models* (Hastie and Tibshirani, 1990) are preferred, because fitting such models circumvents the curse of dimensionality, which tends to render nonparametric regression infeasible in higher dimensions, and because results obtained with such models are particularly easy to visualize, which is important.

Using additive models, the variation in r_t can be decomposed into the variation that can be attributed to each of the state and input variables in turn, and the result can be visualized by means of partial dependence plots with associated bootstrap confidence intervals (Hastie *et al.*, 2001). In this manner, it may be possible to reveal the true structure of the function describing r_t, i.e.:

$$r_t = \varphi_{\text{true}}(\boldsymbol{x}_t, \boldsymbol{u}_t, \boldsymbol{\theta}) \tag{7}$$

which in turn provides the model maker with valuable information about how to re-formulate the incorrect phenomena models or constitutive equations of the model for the next modelling cycle iteration. Needless to say, this should be done in accordance with physical insights.

A more elaborate discussion of the proposed methodology is given by Kristensen *et al.* (2002*a*).

3. CASE STUDY: MODELLING A FED-BATCH BIOREACTOR

To illustrate the performance of the proposed methodology in terms of improving the quality of a model, a simple simulation example is considered in the following. The process considered is a fed-batch bioreactor, where the true model used to simulate the process is given as follows:

$$\frac{dX}{dt} = \mu(S)X - \frac{FX}{V} \tag{8}$$

$$\frac{dS}{dt} = -\frac{\mu(S)X}{Y} + \frac{F(S_F - S)}{V} \tag{9}$$

$$\frac{dV}{dt} = F \tag{10}$$

where X and S are the biomass and substrate concentrations, V is the volume, F is the feed flow rate, $Y = 0.5$ is the yield coefficient of biomass and $S_F = 10$ is the feed concentration of substrate. $\mu(S)$ is the biomass growth rate, described by Monod kinetics and substrate inhibition, i.e.:

$$\mu(S) = \mu_{\max}\frac{S}{K_2S^2 + S + K_1} \tag{11}$$

where $\mu_{\max} = 1$, $K_1 = 0.03$ and $K_2 = 0.5$. Using $(X_0, S_0, V_0) = (1, 0.2449, 1)$ as initial states, simulated data sets from two batch runs (101 samples each) are generated by perturbing the feed flow rate along a pre-determined trajectory and subsequently adding Gaussian measurement noise to the appropriate variables. For the present case it is assumed that all state variables can be measured and noise levels corresponding to variances of 0.01, 0.001 and 0.01 (absolute values) are used.

3.1 First modelling cycle iteration

It is assumed that an initial model corresponding to (8)-(10) has been set up, where the true structure of $\mu(S)$ is unknown. As the first step, this model is then translated into a stochastic grey-box model, which has the following system equation:

$$d\begin{pmatrix} X \\ S \\ V \end{pmatrix} = \begin{pmatrix} \mu X - \dfrac{FX}{V} \\ -\dfrac{\mu X}{Y} + \dfrac{F(S_F - S)}{V} \\ F \end{pmatrix} dt + \boldsymbol{\sigma} d\boldsymbol{\omega}_t \tag{12}$$

where $\boldsymbol{\sigma}$ is a diagonal matrix with elements σ_{11}, σ_{22} and σ_{33}. Since the true structure of $\mu(S)$ is unknown, a constant growth rate μ has been assumed, and a diagonal parameterization of the diffusion term has been used to allow possible model deficiencies to be pinpointed. The model also has the following measurement equation:

$$\begin{pmatrix} y_1 \\ y_2 \\ y_3 \end{pmatrix}_k = \begin{pmatrix} X \\ S \\ V \end{pmatrix}_k + \boldsymbol{e}_k \tag{13}$$

with $\boldsymbol{e}_k \in N(\boldsymbol{0}, \boldsymbol{S})$, where $\boldsymbol{S}$ is a diagonal matrix with elements S_{11}, S_{22} and S_{33}. As the next step, the unknown parameters of the model are estimated using the data from batch no. 1, which gives the results shown in Table 1, and, to evaluate the quality of the resulting model, a pure simulation comparison is performed as shown in Figure 2a. The results of this show that the model does a very poor job, and it is therefore falsified, which means that the modelling cycle must be repeated by re-formulating the model.

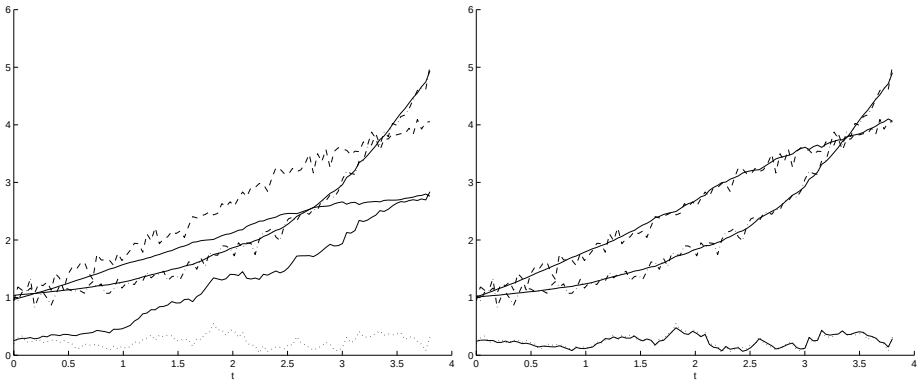

(a) Model structure in (12)-(13). (b) Model structure in (15) and (13).

Fig. 2. Pure simulation comparison using cross-validation data from batch no. 2. Dashed lines: y_1, dotted lines: y_2, dash-dotted lines: y_3, solid lines: pure simulation values.

To obtain information about how to re-formulate the model in an intelligent way, model deficiencies should be pinpointed, if possible. Table 1 also includes t-scores for performing marginal tests for significance of the individual parameters, which show that, on a 5% level, only one of the parameters of the diffusion term is insignificant, viz. σ_{33}, whereas σ_{11} and σ_{22} are both significant. This indicates that the first two elements of the drift term may be incorrect. These both depend on μ, which is therefore an obvious deficiency suspect.

To avoid jumping to conclusions, the suspicion should be confirmed, which is done by re-formulating the model with μ as an additional state variable, which yields the system equation:

$$d\begin{pmatrix} X \\ S \\ V \\ \mu \end{pmatrix} = \begin{pmatrix} \mu X - \dfrac{FX}{V} \\ -\dfrac{\mu X}{Y} + \dfrac{F(S_F - S)}{V} \\ F \\ 0 \end{pmatrix} dt + \boldsymbol{\sigma}^* d\boldsymbol{\omega}_t \quad (14)$$

where $\boldsymbol{\sigma}^*$ is a diagonal matrix with elements σ_{11}, σ_{22}, σ_{33} and σ_{44}, and, since μ has been assumed constant, the last element of the drift term is zero. The measurement equation is the same as in (13). Estimating the parameters of this model, using the same data set as before, gives the results shown in Table 2, and inspection of the t-scores for marginal tests for insignificance now show that, of the parameters of the diffusion term, only σ_{44} is significant on a 5% level. This in turn indicates that there is substantial variation in μ and thus confirms the suspicion that μ is deficient.

As the next step the re-formulated model in (14) and (13) and the parameter estimates in Table 2 are used to obtain state estimates $\hat{X}_{k|k}$, $\hat{S}_{k|k}$, $\hat{V}_{k|k}$, $\hat{\mu}_{k|k}$, $k = 0, \ldots, N$, by means of the EKF, and an additive model is then fitted to reveal the true structure of the function describing μ by means of estimates of possible functional relations between μ and the state and input variables.

It is reasonable to assume that μ does not depend on V and F, so only functional relations between $\hat{\mu}_{k|k}$ and $\hat{X}_{k|k}$ and $\hat{S}_{k|k}$ are estimated, giving the results shown in Figure 3. These plots indicate that $\hat{\mu}_{k|k}$ does not depend on $\hat{X}_{k|k}$, but is highly dependent on $\hat{S}_{k|k}$, which in turn suggests to replace the assumption of constant μ with an assumption of μ being a function of S. More specifically, this function should comply with the functional relation revealed in Figure 3b.

Table 1. Estimation results - (12)-(13).

Parameter	Estimate	Significant?
X_0	9.6973E-01	Yes
S_0	2.5155E-01	Yes
V_0	1.0384E+00	Yes
μ	6.8548E-01	Yes
σ_{11}	1.8411E-01	Yes
σ_{22}	2.2206E-01	Yes
σ_{33}	2.7979E-02	*No*
S_{11}	6.7468E-03	Yes
S_{22}	3.9131E-04	*No*
S_{33}	1.0884E-02	Yes

Table 2. Estimation results - (14)&(13).

Parameter	Estimate	Significant?
X_0	1.0239E+00	Yes
S_0	2.3282E-01	Yes
V_0	1.0099E+00	Yes
μ_0	7.8658E-01	Yes
σ_{11}	2.0791E-18	*No*
σ_{22}	1.1811E-30	*No*
σ_{33}	3.1429E-04	*No*
σ_{44}	1.2276E-01	Yes
S_{11}	7.5085E-03	Yes
S_{22}	1.1743E-03	Yes
S_{33}	1.1317E-02	Yes

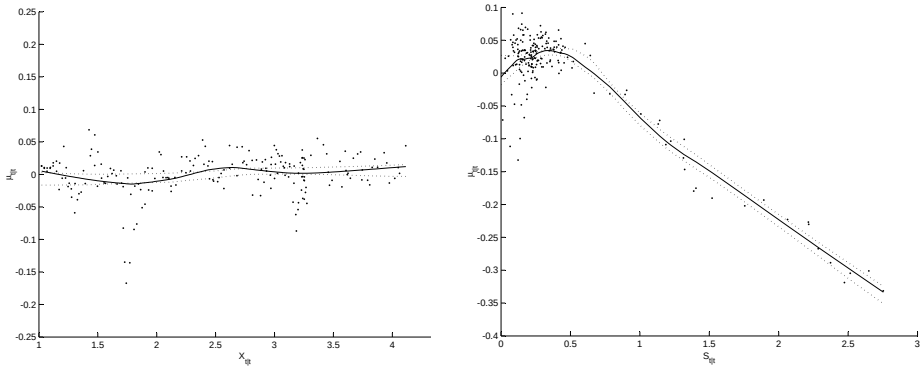

(a) $\hat{\mu}_{k|k}$ vs. $\hat{X}_{k|k}$ (b) $\hat{\mu}_{k|k}$ vs. $\hat{S}_{k|k}$

Fig. 3. Partial dependence plots of $\hat{\mu}_{k|k}$ vs. $\hat{X}_{k|k}$ and $\hat{S}_{k|k}$. Solid lines: Estimates; dotted lines: 95% bootstrap confidence intervals computed from 1000 replicates.

3.2 Second modelling cycle iteration

The functional relation revealed in Figure 3b clearly indicates that the growth of biomass is governed by Monod kinetics and inhibited by substrate, which makes it possible to re-formulate the model in (12)-(13) to yield the system equation

$$d\begin{pmatrix} X \\ S \\ V \end{pmatrix} = \begin{pmatrix} \mu(S)X - \dfrac{FX}{V} \\ -\dfrac{\mu(S)X}{Y} + \dfrac{F(S_F - S)}{V} \\ F \end{pmatrix} dt + \boldsymbol{\sigma} d\boldsymbol{\omega}_t \quad (15)$$

where $\boldsymbol{\sigma}$ is again a diagonal matrix with elements σ_{11}, σ_{22} and σ_{33}, and where $\mu(S)$ is given by (11). The measurement equation remains unchanged and is thus the same as in (13). Estimation of the unknown parameters of this model using the same data set as before gives the results shown in Table 3, and to evaluate the quality of the resulting model, a pure simulation comparison is performed as shown in Figure 2b. The results of this show that the model does a much better job now. It is in fact unfalsified with respect to the available information, and the model development procedure can therefore be terminated.

Table 3. Estimation results - (15)&(13).

Parameter	Estimate	Significant?
X_0	1.0148E+00	Yes
S_0	2.4127E-01	Yes
V_0	1.0072E+00	Yes
$\mu_{\max}$	1.0305E+00	Yes
K_1	3.7929E-02	Yes
K_2	5.4211E-01	Yes
σ_{11}	2.3250E-10	*No*
σ_{22}	1.4486E-07	*No*
σ_{33}	3.2842E-12	*No*
S_{11}	7.4828E-03	Yes
S_{22}	1.0433E-03	Yes
S_{33}	1.1359E-02	Yes

4. CONCLUSION

A systematic framework for improving the quality of first engineering principles models has been presented. The proposed framework is based on stochastic grey-box modelling and incorporates statistical tests and nonparametric regression, which in turn facilitates pinpointing of model deficiencies and subsequent uncovering of their structural origin. A key result is that the proposed framework can be used to obtain estimates of unknown functional relations, which allows unknown or incorrectly modelled phenomena to be uncovered and proper parametric expressions for the associated constitutive equations to be inferred.

REFERENCES

Hastie, T. J. and R. J. Tibshirani (1990). *Generalized Additive Models*. Chapman & Hall. London, England.

Hastie, T. J., R. J. Tibshirani and J. Friedman (2001). *The Elements of Statistical Learning - Data Mining, Inference and Prediction*. Springer-Verlag. New York, USA.

Kristensen, N. R., H. Madsen and S. B. Jørgensen (2002*a*). A method for systematic improvement of stochastic grey-box models. Submitted for publication.

Kristensen, N. R., H. Madsen and S. B. Jørgensen (2002*b*). Parameter estimation in stochastic grey-box models. Submitted for publication.

Raisch, J. (2000). Complex systems - simple models?. In: *Proceedings of the IFAC Symposium on Advanced Control of Chemical Processes* (L. T. Biegler, A. Brambilla, C. Scali and G. Marchetti, Eds.). Elsevier. pp. 275–286.

Young, P. C. (1981). Parameter estimation for continuous-time models - a survey. *Automatica* **17**(1), 23–39.

IDENTIFICATION OF MULTIRATE SAMPLED-DATA SYSTEMS

Jiandong Wang [*] **Tongwen Chen** [*,1] **Biao Huang** [**]

[*] *Dept. of Electrical and Computer Engineering, University of Alberta, Edmonton, AB, Canada T6G 2V4*
[**] *Dept. of Chemical and Material Engineering, University of Alberta, Edmonton, AB, Canada T6G 2G6*

Abstract: This paper studies identification of a general single-input and single-output (SISO) multirate sampled-data system. Using the lifting technique, we associate the multirate system with an equivalent linear time-invariant lifted system, from which a fast-rate discrete-time system is extracted. Uniqueness of the fast-rate system, controllability and observability of the lifted system, and other related issues are discussed. The effectiveness is demonstrated through simulation and a real-time implementation.

Keywords: Multirate sampled-data system, System identification, Controllability and observability, Lifting technique

1. INTRODUCTION

The term Multirate Sampled-Data (MRSD) Systems describes a common phenomena existing in the industry that different variables are sampled at different rates for some reasons (Chen and Qiu, 1994), e.g., a high-purity distillation column (Lee, *et al.*, 1992) and a bioreactor (Gudi, *et al.*, 1995) and CCR octane quality control (Li, *et al.*, 2003). Fig. 1 depicts a SISO MRSD system, where G_c is a continuous-time linear time-invariant (LTI) and causal system with or without a time-delay; H is a zero-order hold with an updating period mh and S is a sampler with period nh, where m, n are different positive integers and h is a positive real number called the base period; discrete-time signals u and y are the system input and output respectively; a continuous-time signal v_c is the unmeasured disturbance. Essentially, it is a linear periodically time-varying (LPTV) system (Kranc, 1957), to which many system identification algorithms cannot be applied directly.

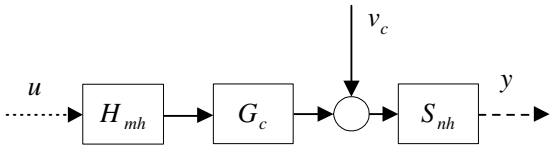

Fig. 1. A SISO multirate sampled-data system

Under such a framework, Lu and Fisher (1988,1989) used an output error method and a least-squares method to estimate intersample outputs based on the fast sampled inputs and slow sampled outputs. Verhaegen and Yu (1994) extended a Multivariable Output Error State Space (MOESP) class of algorithms to identify P subsystems of an LPTV process with period P. Gudi, *et al.* (1995) generated frequent estimates of the primary output based on the secondary outputs and the regular measurement of inputs by an adaptive inferential strategy. Li, *et al.* (2001) identified a fast single-rate model with period mh from multirate input and output data, with an assumption that $m < n$. This work motivates us: Could we do better?

[1] Corresponding author: Telephone: (780)492-3940; Fax: (780)492-1811; Email: tchen@ee.ualberta.ca

Doing better implies two things: first, a fast-rate model with period h instead of mh will be identified; second, a general MRSD system is treated without the assumption $m < n$. Note that our objective includes that of Li, *et al.* (2001), since a model with period mh is readily obtained from a model with period h. The improvement is significant: technically, we need to use additional conditions such as observability of lifted models and coprimeness of the integers m and n (to be clarified later); in terms of applications, the availability of the fast-rate model with period h broadens the choices for multirate control design; the relaxation of assumptions makes identification of fast-rate models for more general MRSD systems possible.

The question states precisely as follows: For a sampling period h, the unknown continuous time system G_c has a discrete time counterpart realized by the step-invariant-transformation, $G_d := S_h G_c H_h$, represented by a state-space model:

$$D + C\left(zI - A\right)^{-1} B = \left[\begin{array}{c|c} A & B \\ \hline C & D \end{array}\right]. \qquad (1)$$

Given the multirate sampled-data system in Fig. 1, how to identify the so-called fast-rate system G_d?

To answer this question, we start in Section 2 with using the lifting technique to associate such an LPTV system with an LTI system, the so-called lifted system. The uniqueness of recovering the fast-rate system from the lifted system is shown in Section 3. Section 4 analyzes controllability and observability of the lifted system, which are essential to the identifiability issues. Section 5 presents two approaches to compute a fast-rate model. Section 6 illustrates the effectiveness of the proposed methods through two examples. We end with some conclusions in Section 7.

2. LIFTING SIGNALS AND SYSTEMS

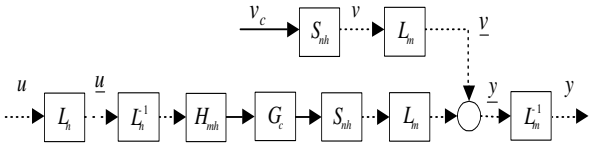

Fig. 2. The lifted multirate sampled-data system

Henceforth, we will focus our discussion on the SISO MRSD system depicted in Fig. 1. Let ψ be a discrete-time signal defined on Z_+ and n be some positive integer. The n-fold lifting operator L_n is defined as the mapping from ψ to $\underline{\psi}$:

$$\left\{\psi(0), \psi(1), \cdots\right\} \mapsto \left\{ \begin{bmatrix} \psi(0) \\ \psi(1) \\ \vdots \\ \psi(n-1) \end{bmatrix}, \begin{bmatrix} \psi(n) \\ \psi(n+1) \\ \vdots \\ \psi(2n-1) \end{bmatrix}, \cdots \right\}.$$

We lift u by L_n into $\underline{u}$, and lift y by L_m into $\underline{y}$. The disturbance v_c is fictitiously sampled into v with period nh, same as the output sampling period, and v is lifted by L_m into $\underline{v}$ (see Fig. 2). Thus, $\underline{u}$, $\underline{y}$ and $\underline{v}$ share the same period mnh, and form a discrete-time LTI system (Francis and Georgiou, 1988):

$$\underline{y} = \underline{G_d}\,\underline{u} + \underline{v} \qquad (2)$$

Here $\underline{G_d}$ is the so-called lifted system from $\underline{u}$ to $\underline{y}$; it has a state space representation by matrices $\underline{A}$, $\underline{B}$, $\underline{C}$ and $\underline{D}$, which are related to A, B, C and D of (1) as shown in Chen and Qiu (1994):

$$\left[\begin{array}{c|c} \underline{A} & \underline{B} \\ \hline \underline{C} & \underline{D} \end{array}\right] := \qquad (3)$$

$$\left[\begin{array}{c|ccc} A^{mn} & \sum_{i=mn-m}^{mn-1} A^i B & \sum_{i=mn-2m}^{mn-m-1} A^i B & \cdots & \sum_{i=0}^{m-1} A^i B \\ \hline C & D_{00} & D_{01} & \cdots & D_{0,n-1} \\ CA^n & D_{10} & D_{11} & \cdots & D_{1,n-1} \\ \vdots & \vdots & \vdots & & \vdots \\ CA^{mn-n} & D_{m-1,0} & D_{m-1,1} & \cdots & D_{m-1,n-1} \end{array}\right]$$

where

$$D_{ij} = D\chi_{[jm,(j+1)m)}(in) + \sum_{r=jm}^{(j+1)m-1} CA^{in-1-r} B \chi_{[0,in)}(r)$$

and a characteristic function on integers is defined:

$$\chi_{[a,b)}(r) = \begin{cases} 1, & a \le r < b \\ 0, & \text{otherwise.} \end{cases}$$

A noise model can be used to further describe the character of the noise term $\underline{v}$ in (2), but it is not within our current objective. Hence, we adopt an output error model structure, since for open loop systems, output error models will give consistent estimates, even if the additive noise is not white (Ljung, 1999). An innovation form of the state-space model with the Kalman filter gain $\underline{K} = 0$ represents the overall discrete-time lifted system:

$$\dot{x} = \underline{A}\,x + \underline{B}\,\underline{u} + \underline{K}\,\underline{e}, \qquad (4)$$

$$\underline{y} = \underline{C}\,x + \underline{D}\,\underline{u} + \underline{e}. \qquad (5)$$

Here overdot denotes one sample advance, $\underline{e}$ is a white noise vector and x is a state vector. If p is the order of G_d, then the dimensions of A, B, C, D are $p \times p$, $p \times 1$, $1 \times p$, and 1×1, respectively, and those of $\underline{A}, \underline{B}, \underline{C}, \underline{D}, \underline{K}$ are $p \times p$, $p \times n$, $m \times p$, $m \times n$, and $p \times m$, respectively. Note that $\underline{A}$ and A share the same dimension.

3. UNIQUENESS OF FAST-RATE SYSTEMS

Before starting the exploration of recovering the fast-rate system from the lifted one, a question

arises naturally: Is the recovery of G_d from $\underline{G_d}$ unique? The answer is affirmative if m and n are coprime. We observe:

$$\begin{aligned}\underline{G_d} &= L_m S_{nh} G_c H_{mh} L_n^{-1} \\ &= L_m S_n \left(S_h G_c H_h\right) H_m L_n^{-1} \\ &= L_m S_n G_d H_m L_n^{-1},\end{aligned} \tag{6}$$

by properties $S_{nh} = S_n S_h$ and $H_{mh} = H_h H_m$, where S_n and H_m are the discrete-time downsampler and the discrete-time zero-order-hold type upsampler respectively. Since the lifting is one-to-one, the problem of recovery of a unique G_d from $\underline{G_d}$ is equivalent to answering a question: Is the mapping $G_d \longmapsto S_n G_d H_m$ one-to-one?

Proposition 1. Assume G_d is LTI and causal. Then, the mapping $G_d \longmapsto S_n G_d H_m$ is one-to-one if and only if m and n are coprime.

Proof:

For sufficiency, it suffices to show that $S_n G_d H_m = 0$ implies $G_d = 0$. Let us assume $S_n G_d H_m = 0$ and let μ be the impulse response of G_d, i.e., $\mu = G_d \delta$, where δ is the discrete-time unit impulse signal. It follows that for any integer i, $S_n G_d H_m U^i \delta = 0$, where U is the unit time-delay operator. This implies, by the definition of H_m,

$$S_n G_d \left(U^{im} + U^{im+1} + \cdots + U^{im+m-1}\right) \delta = 0.$$

The time invariance of G_d and the definition of S_n imply

$$\begin{aligned}&\mu\left(im + jn\right) + \mu\left(im + jn + 1\right) + \cdots \\ &\qquad + \mu\left(im + jn + m - 1\right) = 0,\ \forall i,\ j.\end{aligned} \tag{7}$$

Since m and n are coprime, there exist integers m' and n' such that $mm' + nn' = 1$. Thus, for any k, there always exist $i = km'$ and $j = kn'$ in (7) to get $im + jn = k$. Hence,

$$\mu\left(k\right) + \mu\left(k+1\right) + \cdots + \mu\left(k+m-1\right) = 0, \forall k. \tag{8}$$

By causality of $\mu\left(k\right)$, (8) implies that $\mu\left(k\right) = 0$, $\forall k$, e.g., if $k = -\left(m-1\right)$, then $\mu\left(0\right) = 0$; if $k = -\left(m-2\right)$, then $\mu\left(1\right) = 0$ and so on. Hence, $G_d = 0$.

The necessity is proved as follows. If m and n are not coprime, there exists a common factor k: $m = km', n = kn'$, where m' and n' are coprime. It follows from (6) that $S_n G_d H_m = S_{n'} G_{kd} H_{m'}$ where $G_{kd} = S_{kh} G_c H_{kh}$, i.e., a discrete-time counterpart of G_c with period kh. Thus, the mapping $G_d \longmapsto S_n G_d H_m$ is not one-to-one, since the mapping $G_d \longmapsto G_{kd} = S_k G_d H_k$ is known to be not injective. □

Therefore, in order to get a unique fast-rate system we assume that m and n are coprime. Note that any common factor of m and n can be absorbed into h.

4. LIFTED SYSTEMS

4.1 *Controllability and Observability*

For a state space system to be identifiable, the lifted system $\underline{G_d}$ generally needs to be controllable and observable (Ljung *et al.*, 1999). If the continuous-time system G_c is controllable and observable and the sampling period is non-pathological, then the discrete-time system G_d is also controllable and observable (Kalman, *et al.*, 1963), which is still valid if a continuous time delay exists. Francis and Georgiou (1988) have proved that if G_d is stabilizable and detectable, and satisfies an additional condition $(*)$: For every eigenvalue λ of A, none of the $mn-1$ points

$$\lambda e^{j\frac{2\pi k}{mn}}, k = 1, 2, \cdots, mn-1$$

is an eigenvalue of A, then $\left(A^{mn}, A^i B\right)$ is stabilizable and $\left(CA^i, A^{mn}\right)$ is detectable, for any positive integer i. Based on these, we reach:

Proposition 2. Assume A satisfies the condition $(*)$. If (C, A) is observable, so is $(\underline{C}, \underline{A})$; If (A, B) is controllable and A has no eigenvalues on the unit circle, $(\underline{A}, \underline{B})$ is also controllable.

Proof: The first part follows with some trivial modifications from Francis and Georgiou (1998) in which $\left(CA^i, \underline{A}\right)$ was shown detectable. We prove the second part by showing $\left(\underline{A}, \sum_{i=0}^{m-1} A^i B\right)$ is controllable, i.e., all eigenvalues of $\underline{A}$ are controllable. Now each eigenvalue of $\underline{A}$ has the form λ^{mn}, where λ is an eigenvalue of A. Define functions:

$$g\left(s\right) := \frac{s^{mn} - \lambda^{mn}}{s - \lambda},$$

$$f\left(s\right) := \sum_{i=0}^{m-1} s^i.$$

By non-pathological sampling, $g\left(A\right)$ is invertible (Chen and Francis, 1995). If A has no eigenvalues on the unit circle, then $\sum_{i=0}^{m-1} \lambda^i \neq 0$. Thus $f\left(A\right)$ is invertible. Therefore,

$$\begin{aligned}&\operatorname{rank}\left(\left[\begin{array}{c}\left(A^{mn} - \lambda^{mn} I\right) \sum_{i=0}^{m-1} A^i B\end{array}\right]\right) \\ &= \operatorname{rank}\left(f\left(A\right)\left[\begin{array}{cc} A - \lambda I & B\end{array}\right]\left[\begin{array}{cc} f^{-1}\left(A\right) g\left(A\right) & 0 \\ 0 & I\end{array}\right]\right) \\ &= \operatorname{rank}\left(\left[\begin{array}{cc} A - \lambda I & B\end{array}\right]\right).\end{aligned}$$

Thus, $(\underline{A}, \underline{B})$ is controllable. □

4.2 *Effect of Time Delays*

If there exists a continuous time delay τ larger than h, A has at least two poles at $z = 0$ (Åström and Wittenmark, 1997). Thus, the condition $(*)$ is not satisfied. Observability has been shown to be lost and a remedy is proposed by Li, *et al.* (2001), which is summarized below:

First, we can identify an $m \times n$ time-delay matrix Γ from $\underline{u}$, $\underline{y}$ using correlation analysis (Ljung *et al.*, 1999):

$$\Gamma = \begin{bmatrix} l_{00} & l_{01} & \cdots & l_{0,n-1} \\ l_{10} & l_{11} & \cdots & l_{1,n-1} \\ \vdots & \vdots & & \vdots \\ l_{m-1,0} & l_{m-1,1} & \cdots & l_{m-1,n-1} \end{bmatrix}$$

where l_{ij} is the estimated time delay from the j-th input $\underline{u}_j$ to the i-th output $\underline{y}_i$, $i = 0, 1, \cdots, m-1$ and $j = 0, 1, \cdots, n-1$. The relation between l_{ij} and τ is (Li, *et al.*, 2001):

$$(l_{ij} - 1)\, mnh < \tau + jmh - inh \leq l_{ij} mnh. \quad (9)$$

Second, there exists a one-to-one correspondence between Γ and a positive integer k such that τ is estimated as $kh < \hat{\tau} \leq kh + h$ (Sheng, *et al.*, 2003).

Third, since m and n are coprime, there exist integers k_1 and k_2 such that

$$k = k_1 m + k_2 n. \quad (10)$$

Then, we shift the measured input data: $u_s[l] = u[l - k_1]$ and shift the measured output data: $y_s[l] = y[l + k_2]$, so that, the time delay between u_s and y_s is not larger than h. Hence, controllability and observability will be preserved.

4.3 *Causality Constraint*

Lifting causes a causality constraint, i.e., $\underline{D}$ in (3) is lower triangular. How to identify a model under such a constraint? A modified sub-space identification algorithm was proposed by Li, *et al.* (2001). As an easier alternative, a structured state-space model with free parameters (Ljung, 2001) can be used to deal with the constraint. For instance, if $m = 2$ and $n = 3$, $\underline{D}$ will be parameterized as:

$$\begin{bmatrix} 0 & 0 & 0 \\ \times & \times & 0 \end{bmatrix},$$

where $\times$ marks an adjustable parameter.

5. FAST-RATE MODEL COMPUTATION

Once $\underline{G_d}$ is estimated, how to extract matrices A, B, C? Note $D = 0$ if G_c is causal. The difficulty lies in that in general A cannot be determined by taking the mn-th roots of $\underline{A}$. Once $\hat{A}$, an estimation of A, is known, B and C can be determined as:

$$\hat{C} = C_1, \hat{B} = \left(\sum_{i=0}^{m-1} \hat{A}^i \right)^{-1} B_n$$

where $\underline{B}$, $\underline{C}$ are partitioned as:

$$\underline{B} = \begin{bmatrix} B_1 & B_2 & \cdots & B_n \end{bmatrix}, \quad (11)$$

$$\underline{C} = \begin{bmatrix} C_1^T & C_2^T & \cdots & C_m^T \end{bmatrix}^T. \quad (12)$$

Here the dimensions of B_1, B_2, $\cdots$, B_n are $p \times 1$ and those of C_1, C_2, $\cdots$, C_m are $1 \times p$ and p is the order of the estimated fast-rate model. Note that the proof of *Proposition 2* shows the existence of the inverse.

We propose two approaches to compute A. The first approach, the controllability and observability approach, is based on assumptions that (A_{mh}, B_{mh}) is controllable and (C, A_{nh}) is observable, where

$$A_{mh} := A^m, A_{nh} := A^n,$$

$$B_{mh} := B_n = \sum_{i=0}^{m-1} A^i B.$$

Similar to the proof of *Proposition 2*, both assumptions can be shown to be valid if the conditions in *Proposition 2* are true.

Step 1: Given $\underline{A}$ and $\underline{B}$ in (11), (3) implies

$$A_{mh}^n = \underline{A},$$

$$B_{mh} = B_n, A_{mh} B_{mh} = B_{n-1}, \cdots, A_{mh}^{n-1} B = B_1.$$

Thus, $A_{mh}^k B_{mh}$ is known for any $k \geq 0$. We form the controllability matrix Γ_c of (A_{mh}, B_{mh}) and the shifted controllability matrix Γ:

$$\Gamma_c = \begin{bmatrix} B_{mh} & A_{mh} B_{mh} & \cdots & A_{mh}^{p-1} B_{mh} \end{bmatrix},$$

$$\Gamma = \begin{bmatrix} A_{mh} B_{mh} & A_{mh}^2 B_{mh} & \cdots & A_{mh}^p B_{mh} \end{bmatrix}.$$

Since $A_{mh} \Gamma_c = \Gamma$ and the controllability assumption implies that Γ_c is full row rank, A_{mh} is uniquely determined by

$$\hat{A}_{mh} = \Gamma \Gamma_c^T \left(\Gamma_c \Gamma_c^T \right)^{-1}.$$

Step 2: Given $\underline{A}$ and $\underline{C}$ in (12), (3) implies

$$A_{nh}^m = \underline{A},$$

$$C = C_1, CA_{nh} = C_2, \cdots, CA_{nh}^{m-1} = C_m.$$

Thus, CA_{nh}^k is known for any $k \geq 0$. We form the observability matrix Ψ_o of (C, A_{nh}) and the shifted observability matrix Ψ:

$$\Psi_o = \begin{bmatrix} C \\ CA_{nh} \\ \cdots \\ CA_{nh}^{p-1} \end{bmatrix}, \Psi = \begin{bmatrix} CA_{nh} \\ CA_{nh}^2 \\ \cdots \\ CA_{nh}^{p} \end{bmatrix}.$$

Since $\Psi_o A_{nh} = \Psi$ and the observability assumption implies that Ψ_o is full column rank, A_{nh} is uniquely determined by

$$\hat{A}_{nh} = \left(\Psi_o^T \Psi_o\right)^{-1} \Psi_o^T \Psi.$$

Step 3: Now, $A_{mh} = A^m$ and $A_{nh} = A^n$ are estimated. Since m and n are coprime, there exist two integers $m^{'}, n^{'}$ such that

$$nn^{'} - mm^{'} = 1.$$

Thus, we have:

$$(A_{mh})^{m^{'}} A = (A_{nh})^{n^{'}}.$$

Therefore,

$$\hat{A} = \left(\hat{A}_{mh}^{m^{'}}\right)^{\dagger} \left(\hat{A}_{nh}\right)^{n^{'}}.$$

where $\dagger$ denotes a pseudo-inverse.

The second approach, the matrix roots approach, is based on a condition that $\underline{A}$ is diagonalizable, i.e.,

$$P^{-1} \underline{A} P = \mathrm{diag}\left(\lambda_1, \lambda_2, \cdots, \lambda_p\right).$$

Since $\underline{A} = A^{mn}$, A and $\underline{A}$ share same eigenvectors. If $\rho_i = \alpha_i + j\beta_i$ is a pole of G_c, then

$$\lambda_i = e^{mnh\rho_i} = e^{mnh\alpha_i} e^{jmnh\beta_i}.$$

Assume $|mnh\beta_i| < \pi$ for $i = 1, \cdots, p$.

$$A = P\,\mathrm{diag}\left(\lambda_1^{\frac{1}{mn}}, \lambda_2^{\frac{1}{mn}}, \cdots, \lambda_p^{\frac{1}{mn}}\right) P^{-1}$$

where $\lambda_i^{\frac{1}{mn}}$ is the principal n-th root of λ_i; if this condition is not true, A can be found by searching through all mn-th roots of $\underline{A}$.

6. EXAMPLES

Example 1:

For a system depicted in Fig. 3, take the process and noise model to be

$$G_c(s) = \frac{1}{20s^2 + 4s + 1} e^{-5s}, N_c(s) = \frac{1}{10s + 1}$$

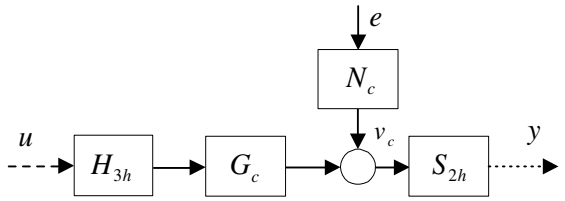

Fig. 3. A SISO MRSD system simulation diagram

and $m = 3$, $n = 2$, $h = 1$ sec. We generate a low frequency random binary signal (RBS) as the input signal u. e is a white noise. The signal-to-noise ratio (SNR) is 3 : 1. The identification procedure is: First, we estimate the time delay as 6 sec and shift the measured output and input data as described in Section 4.2; second, we lift the shifted data to form the lifted signals with a time delay no larger than h; next, based on the lifted signals, we choose a 2nd order lifted model $\underline{\hat{G}_d}$ and compute a fast-rate model $\hat{G}_d$ with period h; finally, we incorporate the estimated time delay. Fig. 4 compares step responses of the actual system G_d and the estimated fast-rate models $\hat{G}_d$. The models are obtained through the proposed approaches: the controllability and observability approach and the matrix roots approach. Both achieve satisfactory results.

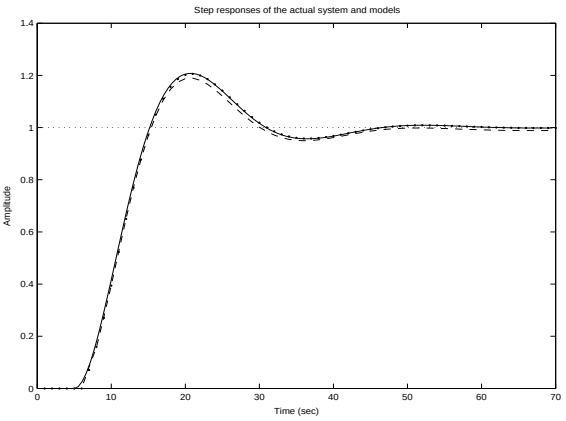

Fig. 4. Step responses of the actual system (solid) and the estimated fast-rate models by the controllability and observability approach (dash) and the matrix roots approach (dotted)

Example 2:

The experiment [2] is implemented on a pilot-scale process in the compute process control laboratory at the University of Alberta. It is a SISO system with the manipulated input u as the cold water valve position and the measured output y as the tank water level. Both are represented by currents (mA), which have linear relationships with the physical units. Around an operating point $u = 11$

[2] Data and Matlab programs are available online. http://www.ee.ualberta.ca/∼jwang/paper.html

mA and $y = 10.3$ mA, a RBS input with a limiting magnitude of 0.4 mA is designed. The input updating period is 80 sec and the output sampling period is 120 sec. Thus, $m = 2$, $n = 3$ and $h = 40$ sec, a dual configuration to Example 1. With 'cheap' data acquisition, we simultaneously measure the input and output every 40 sec, say, u_f and y_f, to be used later for model validation. Following a similar procedure as Example 1, we choose a 2nd order fast-rate model with period 40 sec, using the matrix roots approach. To validate the model, we take u_f as the model input and estimate the model output, which is compared with y_f in Fig. 5. The model captures the process dynamics and steady states very well.

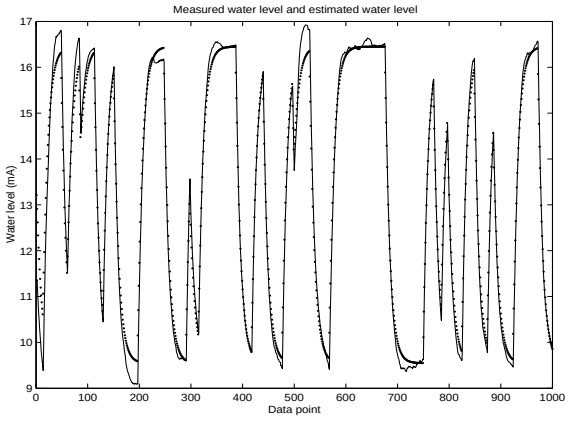

Fig. 5. Comparison of the measured water level (solid) and the estimated water level (dotted)

7. CONCLUSIONS

In this paper, we studied how to estimate a fast-rate model for a general multirate sampled-data system under some mild conditions. The idea is to associate the multirate sampled-data system with an equivalent lifted system, from which the fast-rate model is extracted. Some topics are still open, e.g., how exactly the noise would affect the estimation? how to get an explicit variance expression of the estimated model? These are left to the future investigation.

8. REFERENCES

Åström, K. J. and B. Wittenmark (1997). *Computer-Controlled Systems: Theory and Design*, 3rd ed. Prentice Hall, Englewood Cliffs, N.J.

Chen, T. and L. Qiu (1994). $\mathcal{H}_\infty$ design of general multirate sampled-data control system, *Automatica*, **30**, 1139-1152.

Chen, T. and B. A. Francis (1995). *Optimal Sampled-data Control Systems*, Springer, London.

Francis, B. A. and T. T. Georgiou (1988). Stability theory for linear time-invariant plants with periodic digital controllers, *IEEE Trans. Automat. Control*, **33(9)**, 820–832.

Gudi, R. D., S. L. Shah and M. R. Gray (1995). Adaptive multirate state and parameter estimation strategies with application to a bioreactor, *AIChE Journal*, **41(11)**, 2451-2464.

Kalman, R. and Y. C. Ho and K. Narendra (1963). Controllability of linear dynamical systems, In *Contributions to Differential Equations*, **1**, Interscience, New York.

Kranc, G. M. (1957). Input-output analysis of multirate feedback systems, *IEEE Trans. Automat. Control*, **3**, 21–28.

Lay, D. C. (2000). *Linear algebra and its application*, 2nd ed. Addison-Wesley, Reading, Mass.

Lee, J.H., M.S. Gelormino and M. Morari (1992). Model predictive control of multi-rate sampled-data systems: a state-space approach, *Int. J. Control*, **55(1)**, 153–191.

Li, D., S. L. Shah and T. Chen (2001). Identification of fast-rate models from multirate data, *Int. J. Control*, **74(7)**, 680–689.

Li, D., S. L. Shah, T. Chen and K. Qi (2003). Application of dual-rate modeling to CCR octane quality inferential control, *IEEE Trans. on Control Systems Tech.*, **11(1)**, 43–51.

Ljung, L. (1999). *System identification: Theory for the User*, 2nd ed. Prentice Hall, Englewood Cliffs, N.J.

Ljung, L. (2001). *The System Identification Toolbox: The Manual,* 5th ed. The MathWorks Inc, Natick, MA.

Lu, W. and D. G. Fisher (1988). Output estimation with multirate sampling, *Int. J. Control*, **48(1)**, 149–160.

Lu, W. and D. G. Fisher (1989). Least-squares output estimation with multirate sampling, *IEEE Trans. Automat. Control*, **34(6)**, 669–672.

Sheng, J., T. Chen and S. L. Shah (2003). Time-delay estimation with multirate systems based on interactor matrices, to appear in *Proc. of DCDIS Conf. Engineering Applications and Computational Algorithms*, Guelph, Canada.

Verhaegen, M. and X. Yu (1994). A class of subspace model identification algorithms to identify periodically and arbitrarily time-varying systems, *Automatica*, **31(2)**, 201–216.

SYSTEM IDENTIFICATION FROM MULTI-RATE DATA

R. Bhushan Gopaluni * **Harigopal Raghavan** *
Sirish L. Shah *

* *Department of Chemical & Materials Engineering, University of Alberta, Edmonton, AB, CANADA - T6G 2G6*

Abstract: In this paper, we provide a novel iterative identification algorithm for multi-rate sampled data systems. The procedure involves, as a first step, identifying a simple initial model from multi-rate data. Based on this model, the "missing" data points in the slow sampled measurements are estimated following the expectation maximization approach. Using the estimated missing data points and the original data set, a new model is obtained and this procedure is repeated until the models converge. An attractive feature of the proposed method lies in its applicability to irregularly sampled data. An application of the proposed method to an industrial data set is also included.

Keywords: identification, multi-rate processes, expectation maximization algorithm

1. INTRODUCTION

Traditional identification methods assume that the data are sampled at uniformly spaced sample instants. There is extensive literature on identification of processes from such data (Ljung (1999)). However, in many chemical processes it is either not physically possible to measure certain variables at regular intervals or it is impractical to have frequent or rapid lab assays done. For instance, estimating the composition of the distillate in a distillation column generally takes a few minutes while control moves are implemented at much smaller sample intervals. Such processes with differing sample times for the measured variables are termed multi-rate processes in the rest of this paper. In particular, identification of models for multi-rate processes at the fastest sample rate is the subject of this paper. We refer to the fastest sample rate as the base sample rate and the unavailable data points in the slowly sampled measurements as *missing data*. This allows us to accommodate systems in which outputs are irregularly sampled within the same identification scheme.

A commonly used approach for the identification of processes from multi-rate data is to interpolate between available sampled data. Techniques such as linear or quadratic interpolation are used. Interpolations of these types do not take into account the variation in the input during the period over which the interpolations are made. There have also been attempts at solving the multi-rate identification problem using lifting techniques (Li et al. (2001)). The lifting operator is used to convert the multi-rate identification problem into a multivariable identification problem. However, applying these techniques towards process identification in chemical industries is not easy because the difference in the sampling rates is generally large. For example, (input to output) sampling ratios of $1:15$ are common and estimation techniques to identify a 15-input 'lifted' process would have to be considered. Hence, for processes with a number of inputs and/or large output to input sampling ratios, the identification problem using lifting techniques can become unmanageable. In addition, these techniques are incapable of handling irregularly sampled data.

In this paper we present a method which uses an initial crude model to estimate the unavailable data points in the slowly sampled variables. The estimated unavailable data points are then used with original data set to identify a new model. From the new model,

the missing data is again estimated and this process is repeated until the models converge. This approach reduces to the *Expectation Maximization* (EM) algorithm if optimal estimates of the missing data points are used in the estimation stage. The advantage of this method lies in the methodical manner in which the missing data points are estimated instead of using the traditional interpolation methods. Instead of interpolating, the missing data are estimated based on the current estimate of the process model at each iteration. Use of the EM algorithm guarantees convergence and consistency of the identified models (Dempster et al. (1977)).

The rest of this paper is organized as follows: section 2 lists the assumptions and the notation. In section 3, the EM algorithm is presented and in section 4 a method for identification of linear dynamical systems using the EM approach is developed. In section 5 the EM based identification method is extended to the missing data case. An industrial example is presented in section 6 followed by concluding remarks in section 7.

2. ASSUMPTIONS AND NOTATION

Let us assume that the true process is of the form

$$\begin{aligned} x_{t+1} &= Ax_t + Bu_t + w_t \\ y_t &= Cx_t + v_t \end{aligned} \tag{1}$$

where A, B, C are the system matrices and $x_t \in \mathbb{R}^n$ is the n-dimensional state vector. Assume that $u(t) \in \mathbb{R}^m$ and $y(t) \in \mathbb{R}^p$. w_t and v_t are uncorrelated white noise sequences *i*.e.,

$$\begin{aligned} E[w_t w_t^T] = Q\,; E[w_t] = 0 \qquad \forall\, t \\ E[v_t v_t^T] = R\,; E[v_t] = 0 \qquad \forall\, t \\ E[w_t v_t] = 0 \qquad \forall\, t \end{aligned} \tag{2}$$

Let us represent the time series data from $t = 1$ to $t = N$ of any variable by $(.)_{1:N}$. Through out this paper, we will use the following notation for the expected values of various variables,

$$x_t^s := E(x_t | Y_{1:s}) \tag{3}$$

and

$$\begin{aligned} P_t^s &:= E(x_t - x_t^s)(x_t - x_t^s)^T \\ P_{t,t-1}^s &:= E(x_t - x_t^s)(x_{t-1} - x_{t-1}^s)^T \end{aligned}$$

In addition, the following assumptions are made:

Assumptions

A1. Inputs are sampled uniformly every T units of time.

A2. Outputs are sampled at $T_1, \cdots, T_n$ respectively.

A3. The input sampling time, T, is assumed to be the smallest sampling time *i.e.,*

$$T \leq T_i \qquad \forall\ i \tag{4}$$

A4. Assume that the initial state is zero *i.e.,* $x_0 = 0$.

3. THE EM ALGORITHM

The central idea behind the algorithm presented in this paper is to pose the multi-rate identification problem in the maximum likelihood framework and solve for the system matrices. The iterative algorithm presented in this section is based on the popular *Expectation Maximization algorithm*(EM algorithm) developed in Dempster et al. (1977). Before utilizing this algorithm in identifying multi-rate processes, a brief summary of the algorithm is presented below.

The EM algorithm addresses the problem of estimating model parameters under the maximum likelihood framework. More often than not, the maximum likelihood function is a complicated nonlinear function of the unknown parameters. Hence, one of the earliest methods proposed for solving for the optimal parameters was to use the Newton-Raphson method (Gupta and Mehra (1974)). A simpler method based on the EM algorithm was proposed in Shumway and Stoffer (1982).

The EM algorithm can be summarized in the following few steps :

- Obtain an initial estimate of the parameter vector, Θ^0.
- Carry out the following steps at each iteration, k, until convergence:
  - **Expectation (E-step)**: Find the expected value of the complete data log likelihood function(Q-function) given the observed data set and the previously estimated parameter vector, Θ^k.
  - **Maximization (M-step)**: Maximize the Q-function with respect to the parameter vector

The above steps ensure that the log likelihood function of the observed data increases at every iteration. Therefore, the EM algorithm is guaranteed to converge to a local maximum of the likelihood function. This is an important feature of the EM algorithm. However, there are a few drawbacks associated with any iterative algorithm. The EM algorithm can be sensitive to the initial guess and also the rate of convergence can sometimes be extremely slow. In order to avoid problems with a bad initial parameter guess, we identify an initial unbiased FIR model of the process. An example illustrating the use of EM algorithm in estimating models from multi rate data is presented below.

Example 1. Consider an ARX model

$$y(k) = 0.8y(k-1) + 0.3u(k-1) + e(k) \qquad (5)$$

where $e(k)$ is normally distributed white noise with variance $\sigma_e^2 = 0.01$. Let us assume that the output is sampled at every alternate sample instant and that $y(1)$ is known. Then the following identification objective function based on squared prediction errors can be used

$$\begin{aligned} V_N(\theta) &:= \frac{1}{N}\sum_{k=1}^{N} \varepsilon(t,\theta)^2 \\ &= \frac{1}{N}\sum_{k=1}^{N} [y(k) - \theta_2 y(k-1) - \theta_1 u(k-1)]^2 \end{aligned}$$

where N is the data length and $\theta = [\theta_1 \quad \theta_2]^T$. Since only alternate data points are available, the above objective function can not be evaluated. Instead, it is possible to estimate the expected value of the above objective function given the estimate of θ from the previous iteration, $\hat{\theta}^{(j-1)}$ *i.e.,*

$$\begin{aligned} E\left[V_N(\theta)|\hat{\theta}^{(j-1)}, Z_N\right] = E[\frac{1}{N}\sum_{k=1}^{N} [y(k) - \theta_2 y(k-1) \\ -\theta_1 u(k-1)]^2] \end{aligned} \qquad (6)$$

where Z_N denotes all the available data. Now let us consider two cases:
Case I: $y(k)$ is known, then

$$\begin{aligned} &E\,[y(k) - \theta_2 y(k-1) - \theta_1 u(k-1)]^2 = \\ &(y(k) - \theta_1 u(k-1))^2 + \theta_2^2(\hat{\theta}_1^{(j-1)} u(k-2) \\ &+\hat{\theta}_2^{(j-1)} y(k-2))^2 + \theta_2^2\sigma_e^2 \\ &-2(y(k) - \theta_1 u(k-1))\theta_2(\hat{\theta}_1^{(j-1)} u(k-2) \\ &+\hat{\theta}_2^{(j-1)} y(k-2)) \end{aligned} \qquad (7)$$

Case II: $y(k)$ is unknown, then

$$\begin{aligned} &E\,[y(k) - \theta_2 y(k-1) - \theta_1 u(k-1)]^2 = \\ &(\hat{\theta}_1^{(j-1)} u(k-1) + \hat{\theta}_2^{(j-1)} y(k-1))^2 \\ &+\sigma_e^2 + (\theta_1 u(k-1) + \theta_2 y(k-1))^2 \\ &-2(\theta_1 u(k-1) + \theta_2 y(k-1))(\hat{\theta}_1^{(j-1)} u(k-1) \\ &+\hat{\theta}_2^{(j-1)} y(k-1)) \end{aligned} \qquad (8)$$

Using (7) and (8) in (6) it is possible to find the model parameters at the current iteration, j,

$$\theta^{(j)} = \min_{\theta} E\left[V_N(\theta)|\hat{\theta}^{(j-1)}, Z_N\right] \qquad (9)$$

The iterations are performed until the parameters converge. A plot showing the two parameters in this example and the number of iterations is shown in fig.1. The estimated model parameters converge to the true parameters despite missing data. In general, the estimates using the EM algorithm need not converge to the true parameters with finite data sets. However, the estimated parameters converge to the true parameters asymptotically as the data length increases. On the other hand, the least squares model obtained by interpolating the data is $\hat{\theta}_1 = 0.83$ and $\hat{\theta}_2 = 0.24$, which is clearly not the true model. There is a small amount of bias in the estimated model using the interpolated data. In general, the estimated models are biased if arbitrary interpolation methods are used to fill the missing data points. ■

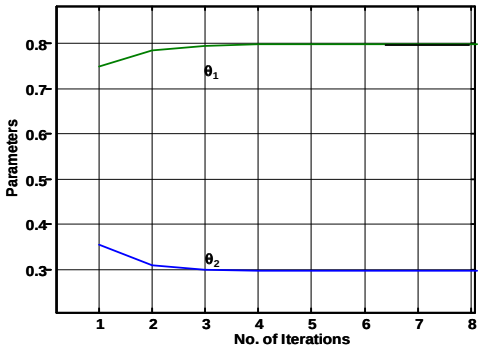

Fig. 1. *Plot of θ_1 and θ_2 as a function of number of iterations*

Now it is possible to use this algorithm to estimate the state matrices of a linear dynamical system described in (1). As a first step we provide an algorithm to estimate the model from the complete data set *i.e.,* there are no missing data. Even though the data set is complete the states are unknown/unobserved and hence the EM algorithm can be utilized. Once a method for identification of single rate systems is developed, it can be extended to multi-rate systems.

4. ESTIMATION OF LINEAR DYNAMICAL SYSTEMS

A maximum likelihood framework is adopted in this section to identify the system matrices of (1). Two independent sequences of noise enter the dynamical system in (1). Hence, the joint log likelihood function of the complete data set can be expressed as

$$\begin{aligned} &\log\mathscr{L}(y_{1:N}, x_{1:N}, \Theta) = \log\mathscr{L}(w_{1:N}, v_{1:N}, \Theta) \\ &= -\frac{N}{2}\log|Q| - \frac{N}{2}\log|R| \\ &-\frac{1}{2}\sum_{t=1}^{N}(x_t - Ax_{t-1} - Bu_{t-1})^T Q^{-1}(x_t - Ax_{t-1} - Bu_{t-1}) \\ &-\frac{1}{2}\sum_{t=1}^{N}(y_t - Cx_t)^T R^{-1}(y_t - Cx_t) \end{aligned}$$

where the parameter vector $\Theta = \{A, B, C, Q, R\}$. The Q-function can then be evaluated by taking the expectation of the log likelihood function given the observed data and parameters from the previous iterate (say Θ^k). Let us define the conditional expectation operator E_k as follows

$$E_k(.) = E(.|y_{1:N}, u_{1:N}, \Theta^k) \tag{10}$$

Now using the above expectation operator the Q-function can be evaluated,

$$\begin{aligned} Q(y_{1:N}, \Theta^k, \Theta) &= -\frac{N}{2}\log|Q| - \frac{N}{2}\log|R| \\ &-\frac{1}{2}\sum_{t=1}^{N} tr\{Q^{-1}E_k(x_t - Ax_{t-1} - Bu_{t-1})(x_t - Ax_{t-1} - Bu_{t-1})^T\} \\ &-\frac{1}{2}\sum_{t=1}^{N} tr\{R^{-1}E_k(y_t - Cx_t)(y_t - Cx_t)^T\} \end{aligned}$$

where $tr(.)$ denotes the trace of a matrix. At each iteration in the EM algorithm a new estimate of the model is obtained by maximizing $Q(y_{1:N}, \Theta^k, \Theta)$ with respect to Θ *i.e.*,

$$\Theta^{k+1} = \max_{\Theta} Q(y_{1:N}, \Theta^k, \Theta) \tag{11}$$

Complete details on obtaining the new estimate, Θ^{k+1} are given in the appendix.

***Example** 2.* Consider the following state space model

$$A = \begin{bmatrix} 0.3688 & 0.4767 & 0.0114 \\ -0.5976 & 0.6095 & -0.5408 \\ -0.0156 & -0.0686 & 0.0422 \end{bmatrix} \quad B = \begin{bmatrix} 0.34 \\ 0.56 \\ 0.78 \end{bmatrix}$$
$$C = [1.2 \quad 0.96 \quad 1.5] \tag{12}$$

with the true covariance matrices

$$Q = \begin{bmatrix} 0.0407 & 0.0001 & 0.0015 \\ 0.0001 & 0.0407 & -0.0020 \\ 0.0015 & -0.0020 & 0.0428 \end{bmatrix}; R = 0.398$$

Using the method proposed in this section one can estimate the model parameters. A plot showing the step responses of the true model, a model obtained using the subspace identification method - N4SID and the model obtained using the EM algorithm are shown in fig.2. The EM algorithm performs as well as the subspace method. The EM algorithm presented in this section, theoretically, will provide asymptotic unbiased estimates. However, in practice the algorithm may not converge fast enough or if a bad initial guess is given, it may converge to a local maximum. Hence, a good initial guess for the EM algorithm is needed. An unbiased least squares model can be used as the initial guess.

■

5. ESTIMATION WITH MISSING DATA

The strength of EM algorithm lies in being able to estimate asymptotically unbiased models even if a portion of the data is missing. As shown in the previous section, it is possible to use the EM algorithm

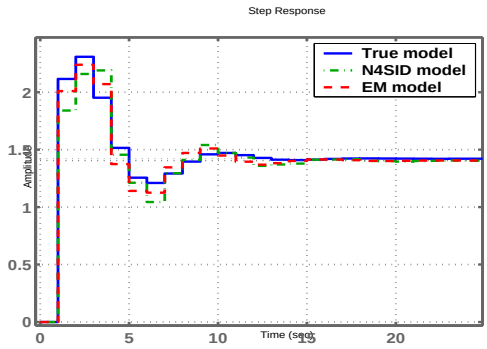

Fig. 2. *Step responses of - the true model, the N4SID model and EM model*

for identification of models from single rate data sets. However, the computational effort involved in using the EM algorithm is too heavy to warrant this method for single rate identification problems. Moreover, traditional identification methods can provide asymptotically unbiased estimates for single rate data sets. On the other hand, in general, identification methods involving arbitrary interpolations to substitute for missing data result in biased estimates; thus, necessitating the development of new methods for identification of models from multi-rate data.

It is interesting to note that the EM algorithm presented in the previous section for identification of linear dynamical systems from single rate data, treats the states as unknown/missing data. Hence, it is possible to extend the same algorithm to include the case of missing data in the outputs by making appropriate changes to the Kalman filter and the Kalman Smoother presented in the Appendix. Full details regarding these modifications can easily be derived along the lines of the arguments given in Shumway and Stoffer (2000).

The procedure can be summarized as follows:

Step 1: Obtain an initial estimate of the model. For instance, it is easy to obtain an FIR model.

Step 2: Estimate the missing data points using the initial estimate of the model. This can be done using the Kalman Filter and the Kalman Smoother.

Step 3: Predict all missing data points using the current model.

Step 4: Using the true and the estimated missing data points identify a new model by minimizing the Q-function.

Step 5: Repeat the above steps until convergence.

***Example** 3.* The process in example 2 is used to generate multi-rate data. The input is sampled every second and the output is sampled every four seconds. Initially, a model is identified using linearly interpolated data and the N4SID algorithm. Then the proposed method is used on the same data set without interpolating the data. The step responses of both the models are shown in fig.3. Clearly, the EM based method outperforms the N4SID method. ■

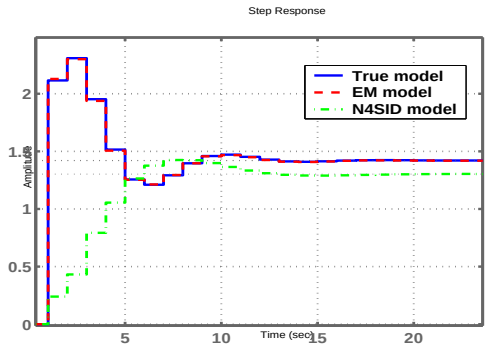

Fig. 3. *Step responses of - the true model, the N4SID model and EM model; Output sampled every four seconds*

6. INDUSTRIAL APPLICATION

In this application, modelling of a mechanical pulp bleaching process at Millar Western, Whitecourt, AB, Canada is shown. The system has four manipulated inputs, two measured disturbance variables and one output. The output, pulp brightness, is an irregularly measured quality variable (distribution of sampling intervals are provided in fig.4). The manipulated in-

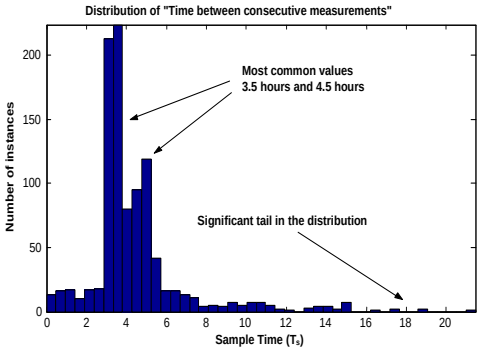

Fig. 4. *Distribution of "time between consecutive measurements"*

puts are chemical add-rates (Peroxide and Caustic) to two towers. The measured disturbances are two wood quality variables (Aspen and Freeness). All inputs are sampled every 10 minutes). The process is known to be a time-delay dominant recycle process. The step responses of the true model have large delay, fast dynamics and recycle characteristics. In general, the presence of a recycle stream can significantly alter the dynamics of a process (Morud and Skogestad (1994),Kwok et al. (2001)). This is especially evident when the process dynamics are faster than the time-delay effects in the process. For example, a step change in one of the inputs in a time-delay dominant recycle process, can cause a staircase-like structure in the output as shown in the fig.5.

When the time-delay in the system is greater than the settling time, including lagged inputs (the extra lags being equal to the sum of the delays in the forward path and the recycle path) as predictors can give a better model. In this particular modelling exercise, there was no provision for performing dynamic tests

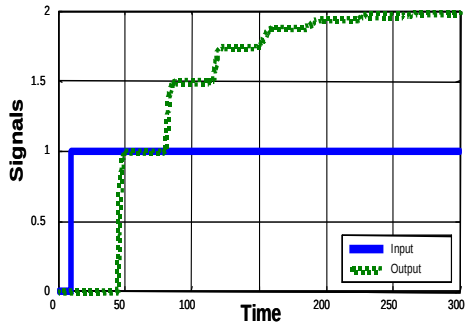

Fig. 5. *Step response of a Delay-dominant recycle process*

to aid model development. Hence we used routine operating data to perform model identification. The routine operating data has enough excitation in the form of grade changes to justify the exercise of model identification using this data.

We used the proposed method based on the EM algorithm for identifying the model. The predictions based on the EM model (without interpolation) and N4SID model (with zero order hold interpolation) are presented in fig.6. The models shown have been adjusted taking the recycle characteristics into account. Hence, only the forward path dynamics are shown. Though it appears that the EM model and the N4SID model perform comparably well for the given data set, it is clear from the step responses (fig.7) that the EM model is representative of the true process dynamics (fast dynamics).

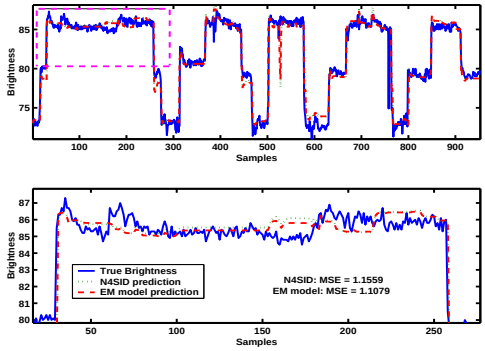

Fig. 6. *Comparison of N4SID and EM model predictions with actual brightness*

7. CONCLUSIONS

An identification approach for multi-rate data, based on the Expectation Maximization approach is presented. Unlike, traditional identification methods for multi-rate data, the proposed method does not use interpolation. An attractive feature of the algorithm is that it can easily handle irregularly sampled data. It leads to asymptotically unbiased estimates of the true model. However, the proposed method is sensitive to the initial guess and is computationally intensive.

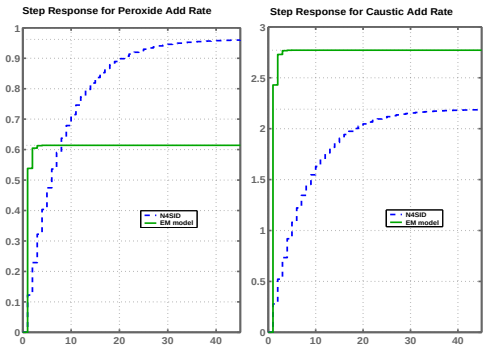

Fig. 7. *Step responses of the N4SID and EM models*

APPENDIX : ESTIMATES OF SYSTEM MATRICES AT EACH ITERATION

Let us first evaluate the second term in the Q-function

$$\begin{aligned} T_2 &:= -\frac{1}{2}\sum_{t=1}^{N} tr\{Q^{-1}E_k(x_t - Ax_{t-1} - Bu_{t-1}) \\ &\quad (x_t - Ax_{t-1} - Bu_{t-1})^T\} \\ &= -\frac{1}{2}tr\{Q^{-1}\left[\Phi_1 + A\Phi_2 A^T + B\Phi_4 B^T + 2\Phi_3 A^T\right. \\ &\quad \left. + 2\Phi_5 B^T - 2A\Phi_6 B^T\right]\} \end{aligned} \tag{A-1}$$

where

$$\begin{aligned} \Phi_1 &:= \sum_{t=1}^{N} E[x_t x_t^T] \quad \Phi_2 := \sum_{t=1}^{N} E[x_{t-1}x_{t-1}^T] \\ \Phi_3 &:= \sum_{t=1}^{N} E[x_t x_{t-1}^T] \quad \Phi_4 := \sum_{t=1}^{N} u_{t-1}u_{t-1}^T \\ \Phi_5 &:= \sum_{t=1}^{N} x_t^N u_{t-1}^T \quad \Phi_6 := \sum_{t=1}^{N} x_{t-1}^N u_{t-1}^T \end{aligned} \tag{A-2}$$

All the expectations are evaluated using the previous model estimate *i.e.*, using $\Theta^k = \{A^k, B^k, C^k, Q^k, R^k\}$. Observe that this is the only term in the Q-function that depends on the system matrices A and B. Now it is straightforward to differentiate the above expression to obtain the optimal estimates of the system matrices at the $(k+1)$th iteration.

$$\begin{aligned} A^{k+1} &= [\Phi_3 - \Phi_5\Phi^{-1}\Phi_6^T][\Phi_2 - \Phi_6\Phi_4^{-1}\Phi_6^T]^{-1} \\ B^{k+1} &= [\Phi_5 - A\Phi_6]\Phi_4^{-1} \end{aligned} \tag{A-3}$$

Similarly we can differentiate the first two terms to obtain the optimal new estimate of the covariance matrix, Q^{k+1}

$$\begin{aligned} Q^{k+1} = \frac{1}{N}\Big[&\Phi_1 + A^k\Phi_2 A^{kT} + B^k\Phi_4 B^{kT} + 2\Phi_3 A^{kT} \\ &+ 2\Phi_5 B^{kT} - 2A^k\Phi_6 B^{kT}\Big] \end{aligned} \tag{A-4}$$

The fourth term in the Q-function can similarly be evaluated,

$$\begin{aligned} T_4 &:= -\frac{1}{2}\sum_{t=1}^{N} tr\{R^{-1}E_k(y_t - Cx_t)(y_t - Cx_t)^T\} \\ &= -\frac{1}{2}tr\{R^{-1}\left[\sum_{t=1}^{N} y_t y_t^T + C\Phi_1 C^T - 2C\sum_{t=1}^{N} x_t^N y_t^T\right]\} \\ &:= -\frac{1}{2}tr\{R^{-1}\left[\Phi_7 + C\Phi_1 C^T - 2C\Phi_8\right]\} \end{aligned} \tag{A-5}$$

Since the matrix C appears only in T_4, the new estimate of C, C^{k+1} can be obtained by differentiating T_4 and equating it to zero.

$$C^{k+1} = \Phi_8^T\Phi_1^{-1} \tag{A-6}$$

In order to obtain an expression for the optimal value of R at the current iteration, we must differentiate the third and fourth term in the Q-function. The new estimate of R can be shown to be

$$R^{k+1} = \frac{1}{N}\left[\Phi_7 - \Phi_8^T\Phi_1^{-1}\Phi_8\right] \tag{A-7}$$

Now we must evaluate all Φ_is. In order to do so, we need to use a Kalman filter and a Kalman smoother. Expressions for the Kalman filter and Kalman smoother provided in Shumway and Stoffer (2000) can be modified to suit the current problem.

REFERENCES

A.P. Dempster, N.M. Laird, and D.B. Rubin. Maximum likelihood from incomplete data via the em algorithm. *J. R. Stat. Soc. B*, 39:1–38, 1977.

N.K Gupta and R.K Mehra. Computational aspects of maximum likelihood estimation and reduction in sensitivity function calculations. *IEEE Trans. Automat. Contr.*, 19:774–783, 1974.

K.E Kwok, M Chong-Ping, and G.A Dumont. Seasonal model based control of processes with recycle dynamics. *Ind. Eng. Chem. Res.*, 40:1633–1640, 2001.

D. Li, S.L Shah, and T Chen. Identification of fast rate models from multi-rate data. *International Journal of Control*, pages 680–689, 2001.

L. Ljung. *System Identification: Theory for the user*. Prentice Hall, 1999.

J Morud and S Skogestad. Effects of recycle on dynamics and control of chemical-processing plants. *comput chem eng*, 18:529–534, 1994.

R.H Shumway and D.S. Stoffer. An approach to time series smooting and forecasting using the em algorithm. *J. Time Series Anal.*,, 3:253–264, 1982.

R.H. Shumway and D.S. Stoffer. *Time Series Analysis and Its Applications*. Springer, 2000.

ROBUST PID TUNING USING CLOSED-LOOP IDENTIFICATION

Yucai Zhu

Control Systems Section, Faculty of Electrical Engineering
Eindhoven University of Technology
P.O. Box 513, 5600 MB Eindhoven, The Netherlands
Phone: +31.40.2473246, email y.zhu@tue.nl

Also at: Tai-Ji Control
Grensheuvel 10, 5685 AG Best, The Netherlands
Phone: +31.499.465692, email: y.zhu@taijicontrol.nl

Abstract: Identification based PID tuning is studied. The proposed approach consists of the identification of linear or nonlinear process model and model based control design. The identification test can be performed in both open loop and closed-loop. The so-called ASYM method is used to solve the identification problem. The method identifies a low order process model with a quantification of model errors (uncertainty). The PID tuning is based on internal model control (IMC) tuning rules. Two case studies will be performed to demonstrate the methodology. The first one is the adaptive control of the dissolved oxygen of a bioreactor; the second one is the nonlinear PID control of a pH process.

Key words: PID control, adaptive control, identification, performance, robustness

1. INTRODUCTION

Although MIMO model based control such as MPC is becoming more popular in process control, most control loops are still PID controllers. PID tuning is also part of the pre-test in an MPC project. Therefore, good tuning of PID loops is very important to maintain good performance of the overall process control system.

PID tuning follows basically two approaches: Manual tuning and model based tuning. Manual tuning is effective for simple loops. The disadvantages are that the quality of the tuning is dependent on the knowledge of the control engineer and the control performance will be, in general, not optimal. Moreover, manual tuning will be difficult and inefficient for processes with complex dynamics and/or nonlinearity. For the control of complex industrial processes, a model-based control approach has been proven the most effective. There are many advantages of a model-based approach. The controller can have a high performance because the controller parameters can be optimized based on the process model. The quality of the tuning is independent of the tuning experience of the control engineer. More complex dynamics can be controlled. Nonlinear processes can be controlled using nonlinear models; time-variant processes can be controlled using an adaptive PID.

In this paper a model based PID auto-tuning method is outlined. The model is identified using open or closed-loop test data. Both linear and block-oriented nonlinear models can be obtained. Model error (uncertainty) is also estimated, which makes the robust tuning possible. Internal model control (IMC) tuning rules (Rivera *et. al*., 1986) are used to determine the PID parameters. In Section 2, the identification method is introduced. Section 3 discusses the controller tuning and implementation. Two case studies are presented in Section 4. Conclusions are given in Section 5.

2. IDENTIFICATION OF LINEAR AND NONLINEAR MODELS

2.1 Cloced-loop Identification of Linear Models

Single-input single-output (SISO) system (process) identification using data from closed-loop operation will be introduced here.

The control system block-diagram is shown in Figure 2.1 where $u(t)$ and $y(t)$ are the process input and output signals at time t, $v(t)$ represents an unmeasured disturbance acting at the output, $r(t)$ is the setpoint of the controlled process. It should be clear that the open loop situation is a special case of closed-loop identification.

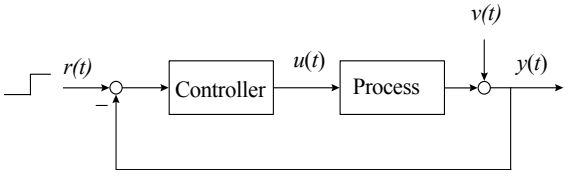

Figure 2.1 Process identification in closed-loop operation

A linear time-invariant discrete-time model that describes the relation between process input and output in terms of the backword shipt operator q^{-1} is given as follows:

$$\begin{aligned} y(t) &= G(q)u(t) + v(t) \\ v(t) &= H(q)e(t) \end{aligned} \qquad (2.1)$$

where

$$G(q) = \frac{B(q)}{A(q)} = \frac{b_0 + b_1 q^{-1} + ... + b_n q^{-n}}{1 + a_1 q^{-1} + ... + a_n q^{-n}}$$

is called process transfer function model, and

$$H(q) = \frac{C(q)}{D(q)} = \frac{1 + c_1 q^{-1} + ... + c_n q^{-n}}{1 + d_1 q^{-1} + ... + d_n q^{-n}}$$

is a disturbance shaping filter, n is called the order of the model, $\{e(t)\}$ is white noise with zero mean and variance λ^2 and

$$\{a_1, \ldots, a_n, b_0, \ldots, b_n, c_1, \ldots, c_n, d_1, \ldots, d_n\}$$

are the parameters of the model. This model structure is called Box-Jenkins model in the literature.

A process identification procedure consists of four steps: test design, parameter estimation, order selection and model validation. The following is the so-called ASYM method (Zhu, 2001) that solves these four problems.

1) Test Design

Often binary test signals are used for linear model identification. Tulleken (1990) has proposed the so-called generalized binary noise (GBN) signal for use in identification. The character of a GBN signal is determined by its power spectrum which is in turn determined by its amplitude and average switch time.

A good test design should meet two requirements: 1) the test signal should excites the process such that the identified model is most accurate for control, 2) the test will not disturb normal production, or, the disturbance is minimized. The spectrum of the test signal should be determined such that the control error of the identified model is minimal. An approximate optimal spectrum formula of the test signal at the setpoint of the closed-loop system is given as (Zhu and van den Bosch, 2000)

$$\Phi_r^{opt}(\omega) \approx \mu\sqrt{\Phi_r(\omega)\Phi_v(\omega)} \qquad (2.2)$$

where $\Phi_r(\omega)$ is the power spectrum of the reference signal r, $\Phi_v(\omega)$ is the power spectrum of the disturbance, and μ is a constant adjusted so that the signal power (or amplitude) is constrained. In practice, the average switch time of the GBN signal is adjusted so that its spectrum approximates the optimal one in (2.2). The amplitude is chosen so that the process output will stay within a given range.

2) Parameter Estimation

Parameters of $G(q)$ and $H(q)$ can be estimated in several ways. The well known prediction error method (Ljung, 1987) estimates the parameters of both $G(q)$ and $H(q)$ by minimizing the *prediction error* criterion according to (2.1). This approach is numerically difficult. Local minima and non-convergence can occur.

In the so-called ASYM method (Zhu, 2001), first a high order ARX (equation error) model is estimated:

$$\hat{A}^h(q)y(t) = \hat{B}^h(q)u(t) + \hat{e}(t) \qquad (2.3)$$

where $\hat{A}^h(q)$ and $\hat{B}^h(q)$ are polynomials.

The high order model in (2.3) is practically unbiased, provided that the process behaves linear around the working point. The variance of this model is high due to its high order. Using the asymptotic result of Ljung (1987) it can be shown that the asymptotic negative log-likelihood function for the reduced process model is given by (Wahlberg, 1989)

$$\int_{-\pi}^{\pi} |\{|\hat{G}^h(e^{i\omega}) - \hat{G}(e^{i\omega})|^2 \frac{\Phi_v(\omega)\lambda^2}{\Phi_u(\omega)\lambda^2 - |\Phi_{ue}(\omega)|^2}|\, \mathrm{d}\omega \qquad (2.4)$$

The reduced model $\hat{G}(q)$ is thus calculated by minimizing (2.4) for a fixed order.

3) Order Selection

The best order of the reduced model is determined using a frequency domain criterion ASYC which is relate to the noise-to-signal ratios and to the test time; see Zhu (2001). The basic idea of this criterion is to equalize the bias error and variance error of the transfer function in the frequency range that is important for control.

If the optimal order is higher than 2, a model reduction is used to reduce the order to 2 for PID tuning.

4) Model Validation

Model validation is to check whether the identified model is suitable for control. The main task of model validation is to check if the identification test data is rich enough for control purpose, and if not, provide a test redesign. In Zhu (2001), a stochastic model error bound has been derived based on the asymptotic properties of high order models. Denote $\Delta(e^{i\omega})$ as the high order model error, then the additive error bound $\bar{\Delta}(\omega)$ is given as:

$$|\Delta(e^{i\omega})| \le \bar{\Delta}(\omega) := 3\sqrt{\frac{n_h}{N}\frac{\Phi_v(\omega)\lambda^2}{\Phi_u(\omega)\lambda^2 - |\Phi_{ue}(\omega)|^2}} \quad \text{w.p. } 99.9\% \quad (2.5)$$

where n_h is the order of the high order model, N is the number of samples, $\Phi_v(\omega)$ is the power spectrum of disturbance, $\Phi_u(\omega)$ is the power spectrum of input, $\Phi_{ue}(\omega)$ is the cross power spectrum between input and white noise sequence $\{e(t)\}$. When the optimal model order is higher than 2, the model order will be reduced to 2. In this case, the difference between the optimal model and the 2nd order model will be added to the upper bound (2.5).

One way to use upper bound (2.5) for model validation is as follows. First simulate the control system using the model and controller. Then check the robust stability of the system using the model, the upper bound and the controller parameters; see Section 3. If the controller simulation show good performance and robust test is passed, the identified model passes the validation and the controller can be implemented. If the robust test is failed, then, according to the upper bound formula (2.5), a test redesign can be done using the following rules:

- *Doubling the test signal amplitude will half the error over the whole frequency band.*
- *Doubling the test time will reduce the error by a factor of 1.414 over the whole frequency band.*
- *Doubling the average switch time of GBN signal will half the error at low frequencies and double the error at high frequencies.*

2.2 Identification of Block-Oriented Nonlinear Models

Commonly used block-oriented models are the Hammerstein model, the Wiener model and combined Hammerstein-Wiener models. A Hammerstein model is formed by a nonlinear gain at the input followed by a linear block, hence it can also be called a N-L model; see Figure 2.2. A linear block followed by a nonlinear gain forms a Wiener model or a L-N model; see Figure 2.3. One way to combine the Hammerstein Model and and the Wiener model is the so-called N-L-N Hammerstein-Wiener model; see Figure 2.4.

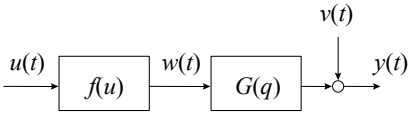

Figure 2.2 Hammerstein model

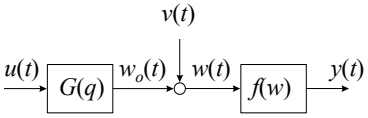

Figure 2.3 Wiener model

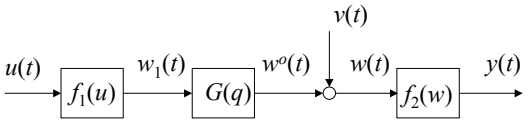

Figure 2.4 N-L-N Hammerstein-Wiener model

Here, $G(z^{-1})$ represents a linear time-invariant transfer function, $f(.)$ denotes the static nonlinear gain. It is assumed that: 1) the nonlinear function $f(.)$ is continuous, monotone and invertible; 2) the unmeasured disturbance $\{v(t)\}$ is a stationary stochastic process.

One can parametrize the linear part with the disturbance using the Box-Jenkins model; and parametrize the nonlinear function using cubic splines. Recently, identification algorithms have been developed for such models by extending the ASYM method; see Zhu (1999, 2000, and 2002).

3. ROBUST PID TUNING

3.1 Tuning for Linear PID

There are many model-based PID tuning rules, such as dominant pole placement, optimization by minimizing *integral square error* (ISE) or *integral absolute error* (IAE), and internal model control (IMC) tuning; see Åström and Hägglund (1995).

Here we will use the IMC tuning rules introduced by Rivera *et. al*. (1986). The idea of the IMC tuning is to use the two-step IMC design method to derive the PID parameters based on a low order (up to 2nd order) plus delay model of the process. The PID parameters are determined so that the closed-loop behavior approximates the behavior given by a first order filter

$$f(s) = \frac{1}{\tau_{cl}s + 1} \quad (3.1)$$

For controller tuning, the user only needs to specify the time constant τ_{cl} of the filter, or the desired speed of the closed-loop system. In general, a large time constant leads to a slow response and a more robust controller; a small time constant leads to a fast response, but a less robust controller. Tuning formulae for typical process models are available in tables; see, e.g., Chien and Fruehauf (1990). Therefore, when a process model is identified, it is

straightforward to obtain PID parameters. The closed-loop system can be simulated using the model and the controller. Industrial experience of the IMC tuning rules is very positive; see Chien and Fruehauf (1990).

Because model errors are inevitable in real process identification, a good control performance according to simulation does not necessarily mean good performance in reality. The robustness of the controlled system against model errors can be analyzed using the upper error bound in (2.5). Denote $\hat{G}(s)$ as the process model in continuous-time, $C(s)$ as the controller and $\overline{\Delta}(\omega)$ as the upper bound. Then it can be shown (see, e.g., Rivera *et. at*.,1986) that the controlled system is robustly stable for all the errors bounded by the upper bound if and only if

$$\frac{|C(i\omega)|}{|1+\hat{G}(i\omega)C(i\omega)|}\cdot\overline{\Delta}(\omega)<1 \quad \forall\omega\in[0,\infty] \qquad (3.2)$$

The performance of the true system will be close to the simulation if the left hand side of (3.2) is much smaller than 1, for example, smaller than 0.5.

3.2 Tuning for Nonlinear PID

When a Hammerstein model or a Wiener model is identified, the simplest tuning is to invert the nonlinearity and then use the same IMC tuning rules to find the linear part of PID controller. The robust stability analysis can also be used after the nonlinear compensation. Denote $\hat{f}^{-1}(.)$ as the identified nonlinear gain, then the block diagram for the nonlinear PID control using the Hammerstein model is given in Figure 3.1; and that using the Wiener model is shown in Figure 3.2.

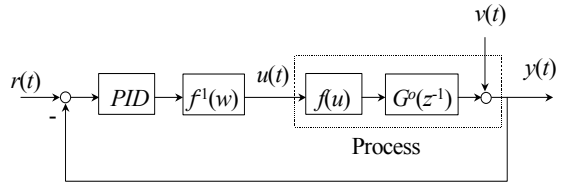

Figure 3.1 Nonlinear PID for Hammerstein model

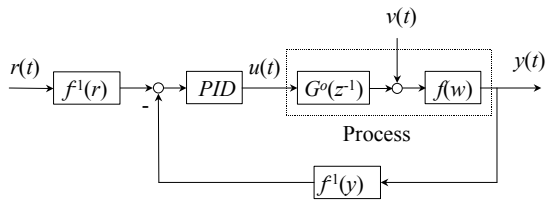

Figure 3.2 Nonlinear PID for Wiener model

4 CASE STUDIES

4.1 Adaptive Control of the Disolved Oxygen of a Bioreactor

The setup is a 20 liter fermentor (Figure 4.1). In this setup, base and acid are used to control the pH value; heating and (water) cooling are used to control temperature and airflow is used to control dissolved oxygen.

The production specifications for the three controlled variables are:

1) **pH** Normal range: setpoint ± 0.05. Worst case range: setpoint ± 0.05.

2) **Dissolved oxygen** Nornal range: setpoint ± 2.0%. Worst case range: setpoint ± 5.0%.

3) **Temperature** Normal range: setpoint ± 0.1 °C. Worst case range: setpoint ± 1.0 °C.

Each variable is controlled using a PID controller. Experience has shown that, when fixed PI controllers are used, the controls of pH and dissolved oxygen are difficult, but the control of temperature is easier.

The main disturbances to the dissolved oxygen are changes in the oxygen consumption rate during the fermentation, the addition of anti-form the changes of the medium properties.

Applikon ADI 1065 unit that is connected to the sensors and actuators controls the fermentor. The low level PID control loops are run in a PC. The supervisory controller sets the PID parameters. The supervisor controller runs in another PC under Matlab/Simulink/ Stateflow. The sampling time is 5 seconds.

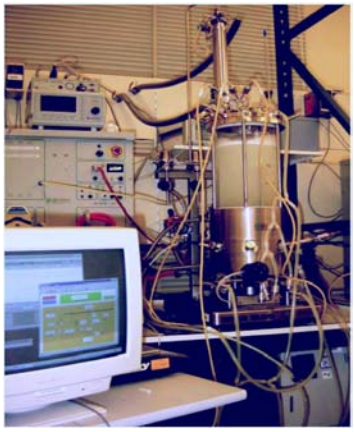

Figure 4.1. The bioreactor setup

The adaptive control scheme is as follows.

1) Control loop performance monitoring
   Is control performance OK?
   Yes, goto 1); no, goto 2)
2) Identification test; identifying model and error bound
3) Performing PID tuning and simulating closed-loop responses
4) Performing robust stability test
   Is the control system robust?
   Yes, goto 5);
   No, goto 2) (for collecting more test data), or, goto 3) (detune the controller)
5) Implement the new PID parameters
   Goto 1)

In this work, control performance monitoring (Huang and Shah, 1999) is not studied; only identification and PID tuning are shown.

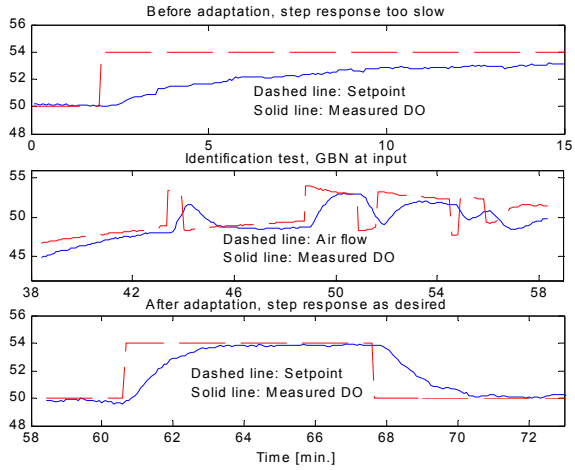

Figure 4.2 DO control loop before, during and after the adaptation

Figure 4.2 shows the signal plots of the real-time measurements during the test. First the existing PID tuning is made very slow; see the first plot of Figure 4.2. Then the identification test is started. A GBN signal is added at the process input. The test lasted for about 20 minutes; see the second plot of Figure 4.2. At the end of the 20 minutes, the input/output data is used to identify a model and its error bound, and PID parameters are computed. The desired settling time of the closed-loop is 1 minute. The closed-loop system is simulated and the robust stability is tested using the model and the control parameters see Figure 4.3. It shows that the new PID controller has good performance with robust stability. The new PID parameters are implemented in the low level controller and the step responses is measured after the adaptation; see the third plot of Figure 4.2.

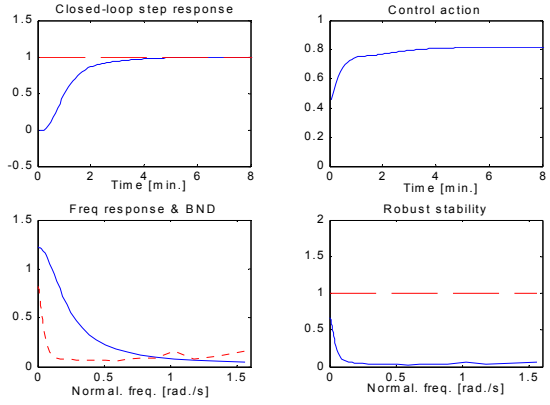

Figure 4.3 Identification and robust PID tuning

It can be seen that the performance of the adaptive control is very satisfactory. The simulation and the real-time measurements agree very well. Only a few seconds are needed to carry out the off-line identification, PID tuning and robust stability analysis.

When the closed-loop is in oscillation, the identified model is very poor. This results in a large error bound and the robust stability test will fail. Therefore the new control parameters will not be implemented. To solve this problem, and oscillation detection is performed before the identification test. The existing controller is detuned until the oscillation disappears.

The adaptive control of the pH and the temperature can be done in the same way.

4.2 Nonlinear PID Control of a pH Process

The pH process consists of a continuous stirred tank reactor (CSTR) with two input streams and one output stream. The scheme is shown in figure 4.4. The first input flow consists of solution of strong acid and the second flow consists of a solution of strong base. The acid flow has a constant rate and the rate of base flow can be adjusted using a controlled pump. These two flows react with each other and produce a pH value. The pH of the solution inside the CSTR is measured by using a pH sensor. The base flow rate is used to control the pH value of the solution inside the tank.

Closed-loop identification test has been carried out. Staircase test signal with different step length is applied at the pH setpoint. Wiener model is identified using the test data. The linear model has an order of 2, but a first order model is almost as good. The nonlinear part has degree 10. Figure 4.4 shows the identified nonlinear gain which decreases as the pH increases.

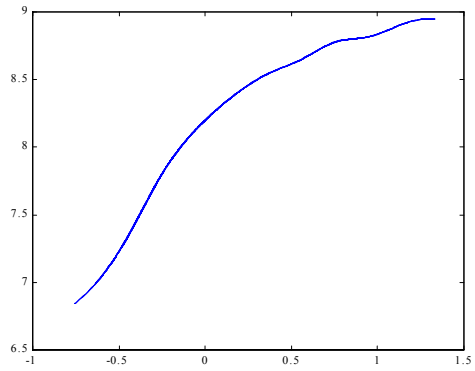

Figure 4.4 Identified nonlinear gain

Based on the identified Wiener model, a nonlinear PID controller is designed and tested for the pH process. In the control scheme, the inverse of the nonlinear gain is placed in the feedback path and before the setpoint as shown in Figure 3.2. Figure 4.5 shows the control result of the nonlinear PID (step responses); Figure 4.6 shows the result of linear PID. One can see that the system with linear controller becomes slower when the pH value is high, but with the nonlinear controller the performance is nearly the same for low and high pH values.

The control scheme is implemented in a LabView environment. See Erol (1999) for more details on the study.

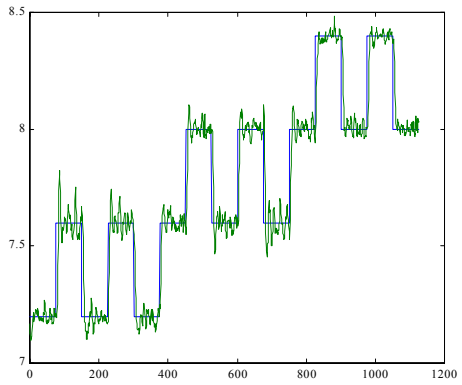

Figure 4.5 Step responses of the nonlinear PI controller

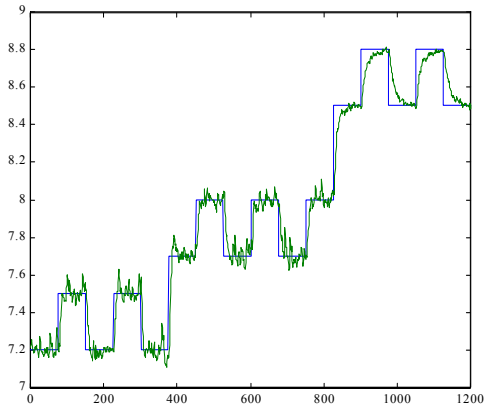

Figure 4.6 Step responses of the linear PI control

5. CONCLUSIONS

An identification based robust PID tuning method is proposed. Both linear and simple nonlinear models can be identified in a possibly closed-loop operation. An error bound of the linear model part can be estimated, which makes the robust tuning possible. The linear or nonlinear PID controller is determined using the so-called IMC tuning rules. The robust stability analysis is then carried out using the identified model, the error bound and the controller parameters. There are many ways to implement the proposed method to solve industrial control problems. The first way is to use the linear method in an auto-tuner to tune fixed PID controllers. The second way is to use the linear identification and PID tuning in an adaptive controller. The third way is to design a time-invariant nonlinear PID controller. The two case studies have shown the capability of the methodology. our experience, the use of such test signals is often permitted in industrial environments.

REFERENCES

Åström, K. and T. Hägglund (1995). *PID Controllers: Theory, Design and Tuning*. Instrument Society of America, Research Triangle Park, NC 27709, USA.

Babuska, R., M.R. Damen, C. Hellinga and H. Maarleveld (2001). Fuzzy supervision of adaptive control with an aaplication to bioreactors. *Journal A*, this issue.

Erol, F. (1999). Nonlinear PID control using Hammerstein or Wiener models. M.Sc. Thesis. Faculty of Electrical Engineering, Eindhoven University of Technology, The Netherlands.

Chien, I.-L. and P.S. Fruehauf (1990). Consider IMC tuning to improve controller performance. *Process Control*. October, 1990, pp 33-41.

Huang B. and S.L. Shah (1999). *Performance Assessment of Control Loops*. Springer-Verlag London.

Rivera, D.E., M. Morari and S. Skogestad (1986). Internal model control 4. PID controller design. *Ind. Eng. Chem. Process Des. Dev.*, Vol. 25, p. 252.

Tulleken, H.J.A.F. (1990). Generalized binary noise test-signal concept for improved identification-experiment design. *Automatica*, Vol. 26, No. 1, pp. 37-49.

Zhu, Y.C. (1999). Parametric Wiener model identification for control. *Proceedings of IFAC Congress*, July 5-9, 1999, Beijing.

Zhu, Y.C. (2000). Hammerstein model identification for control using ASYM. *International Journal of Control*, Vol. 73 No.18 pp. 1692-1702.

Zhu, Y.C. (2001). *Multivariable System Identification for Processes Control*. Elsevier Science, Oxford.

Zhu, Y.C. (2002). Estimation of an N-L-N Hammerstein-Wiener model. *Automatica*. Vol. 38, No. 9, pp 1607-1614.

ESTIMATION OF REACTION RATES BY NONLINEAR SYSTEM INVERSION

Adel Mhamdi and Wolfgang Marquardt [1]

Lehrstuhl für Prozesstechnik, RWTH Aachen

Abstract: The estimation of reaction rates is an important problem in mechanistic modeling, monitoring and control of chemical reactors. In contrast to standard estimation techniques where a model must be chosen for the reaction rates, we consider them in this work as unknown time-varying functions, which also may be interpreted as inputs. The resulting estimation task is an ill-posed inverse problem. The paper addresses this estimation problem based on systematic methods for nonlinear system inversion and filtering resulting in efficient estimators. A theoretical analysis reveals the conditions for reaction rate reconstruction are those for system invertibility. Our estimation scheme is a regularization method which eliminates the difficulties arising with ill-posed problems. Guidelines for the design of the estimator structure and the selection of the regularization parameters are presented.

Keywords: Inverse problems, ill-posed problems, system inversion, filtering, regularization, reaction rates.

1. INTRODUCTION

Reaction rates are important quantities for mechanistic modeling, monitoring and control of chemical reactors. Since these quantities are not often directly measurable, they must be estimated from other measurable quantities, such as temperature, pressure and eventually concentrations. This necessitates however an accurate model of the process, which is rarely available. In reality, the reaction rates are complex functions of unknown structure of the temperature and the concentrations of the reacting species involving many kinetic parameters.

An approach to the estimation of reaction rates, which does not rely on kinetic expressions, has been investigated by Schuler and Schmidt (1992). It has been based on a calorimetric model comprising conservation equations for mass and energy. The estimator used is the Kalman filter. The authors report on estimation of reaction rates, conversion and rate of production and on the use of these quantities to control runaways and overfeeding. The problem has also been considered by Eliçabe *et al.* (1995). The authors use a stationary Kalman filter together with a simple linear model basically derived from the definition of the reaction rate and assuming knowledge of total mass of the reacting species derived from concentration measurements. In order to cast the problem in a form suitable to apply standard Kalman filtering techniques, a model must be chosen to represent the reaction rate (de Vallière and Bonvin, 1990; Eliçabe *et al.*, 1995; Schuler and Schmidt, 1992). In general, estimation results will depend on the model selected (de Vallière and Bonvin, 1990). Hence, the type of model chosen is a degree of freedom of the estimation scheme.

[1] Author to whom all correspondence should be addressed, Turmstr. 46, 52056 Aachen, Germany, phone: +49.241.8096712, fax: +49.241.8092326, email: wma@lfpt.rwth-aachen.de

In our earlier work (Mhamdi and Marquardt, 1999), we have developed an inversion-based regularization for the estimation of reaction rates without assuming any reaction rates model. Instead, the reaction rates have been considered as unknown input functions to be estimated from concentration measurements of the reacting species. Insight into this estimation problem has been gained by noticing that this task is actually an inverse problem, which is roughly defined by determining causes for desired or observed effects (Engl *et al.*, 1996). The solution of inverse problems is generally a difficult task since they are usually *ill-posed* (Engl *et al.*, 1996; Hansen, 1998), i.e. their solution is not unique and/or unstable with respect to data in the sense that small perturbations in the measurements cause large variations in the estimate. Ill-posedness is due to the smoothing character inherent to causal relations. Different causes, even well-separated, may result in almost an equal or the same effect.

In this paper, we consider the extension of our previous method (Mhamdi and Marquardt, 1999) to deal with MIMO linear and nonlinear systems. Our estimation scheme is based on regularization techniques (see e.g. Engl *et al.* (1996) for a review), which deal with the difficulties arising due to the ill-posedness of such problems. In general terms, regularization refers to the approximation of an ill-posed problem by a parameter dependent family of neighboring well-posed problems. Examples are Tikhonov regularization (Tikhonov and Arsenin, 1977) and regularization by projection (Kirsch, 1996). The inversion approach gives important insight into the inherent properties of the estimation problems and, in particular, the error trade-off to get the best solution.

The paper is organized as follows. The problem formulation and the solution framework are stated in Section 2 and 3 respectively. The design procedure based on system inversion for unknown input estimation is given for linear and nonlinear MIMO systems in Section 4. In Section 5, the case study of a bioreactor is presented. Conclusions are given in Section 6.

2. INPUT ESTIMATION PROBLEM

We consider in this work systems Σ_{NL} given by the following nonlinear equations

$$\dot{x}(t) = A(x) \; + \; B(x) \; w(t), \tag{1}$$

$$y(t) = C(x) \; + D(x) \; w(t) \tag{2}$$

where the quantities w and y are vector-valued functions, i.e. $w(t) \in \mathbb{R}^m$ and $y(t) \in \mathbb{R}^p$ for $t \in [t_0, t]$ and $x(t) \in \mathbb{R}^n$ are the system states. The quatities $w(t)$ represent the unknown inputs to be estimated from measurements of the outputs y. In the application context considered these inputs are the reaction rates of interest.

Since the observations are always corrupted with errors, the measurements, denoted by $\tilde{y}$, are different from the true values y. We assume that the two quantities are related through the following equation

$$\tilde{y}(t) = y(t) + n(t), \tag{3}$$

in which n represents an additive measurement error.

We formulate the problem as follows. Let $T_{w \to y}$ be the operator mapping the unknown input vector $w \in \mathbb{W}$ to the measured output $y \in \mathbb{Y}$, i.e.

$$T_{w \to y} \; w = y \tag{4}$$

The sets $\mathbb{W}$ and $\mathbb{Y}$ are function spaces. The input-output operator $T_{w \to y}$ is implicitly given by the system Σ_{NL}.

The unknown input estimation (UIE) problem is to find an approximation $\hat{w}$ of the unknown input functions $\{w(\tau), \tau \in [t_0, t]\}$ from the noisy observations $\{\tilde{y}(\tau), \tau \in [t_0, t]\}$. In other words, the estimation problem is to solve the integral equation (4) for w using the available noisy measurements $\tilde{y}$, i.e.

$$T_{w \to y} \; w = \tilde{y}, \tag{5}$$

3. SOLUTION FRAMEWORK

In this work, we approach the UIE problem from the perspective of inverse problems and regularization theory. In general the UIE problem is ill-posed, which means that one or more of the following well-posedness properties, due to Hadamard (Engl *et al.*, 1996), does not hold: (i) for all admissible data a solution exists, (ii) for all admissible data the solution is unique and (iii) the solution is stable. Of major concern is the stability condition, which means, that the solution must depend continuously on the data such that small perturbations in the data cause small variations in the solution.

The standard method to guarantee the solution existence and uniqueness for problem (5) is to consider generalized solutions denoted by $w^\dagger$ (Engl *et al.*, 1996). In the L_2-norm, $w^\dagger$ is the *minimum norm least-squares solution* of the integral equation (5). The generalized inverse operator $T^\dagger$ maps y to $w^\dagger$. The generalized solution $w^\dagger$ may be hence determined through

$$w^\dagger = T^\dagger \tilde{y}. \tag{6}$$

However, the usefulness of this solution depends strongly on the properties of the inverse operator $T^\dagger$, i.e. its continuity. Therefore, within the UIE problem, we are interested in the inverse operator and its properties.

The generalized inverse is generally unbounded such that stability cannot be guaranteed. Regularization methods are used to recover this property of the solution. A regularization method is a family of well-posed transformations T_α, such that

$$\lim_{\alpha \to 0} T_\alpha y = T^\dagger y, \quad \forall\ y, \tag{7}$$

where α is called the *regularization parameter* (Engl *et al.*, 1996; Tikhonov and Arsenin, 1977). In other terms, the introduction of regularization is connected to the approximation of the inverse operator in the family of continuous operators.

Regularization, however, introduces an extra error term to the estimate. To see this, consider measurements satisfying

$$\|\tilde{y} - y\| \leq \epsilon, \tag{8}$$

where ϵ is an error level. For any bounded linear operator T_α, the error in the regularized solution $w_\alpha^\epsilon = T_\alpha \tilde{y}$ can be calculated according to

$$\hat{w}_\alpha^\epsilon - w^\dagger = T_\alpha \tilde{y} - T^\dagger y \tag{9}$$

$$= T_\alpha(\tilde{y} - y) + (T_\alpha - T^\dagger)y. \tag{10}$$

The term $T_\alpha(\tilde{y} - y)$ is called *data error* and $(T_\alpha - T^\dagger)y$ *regularization* or *approximation error*. As a function of α these two error types have different behavior, such that the minimization of the total error results in a trade-off between them. No regularization method is therefore complete without a procedure for choosing the regularization parameter α.

4. REGULARIZATION BY SYSTEM INVERSION AND FILTERING

In our earlier work, a filter-based regularization, originally investigated in (Tikhonov and Arsenin, 1977) for SISO problems, has been developped for the solution of inverse heat conduction problems (Blum and Marquardt, 1997) and the estimation of reaction rates in chemical reactors (Mhamdi and Marquardt, 1999). In the following section, we consider the extension of the method for MIMO linear and nonlinear systems.

4.1 Linear systems

We consider the operator $T_{w \to y}$ given by the MIMO LTI system Σ_L

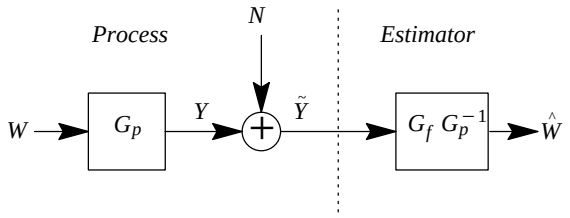

Fig. 1. Filter-based regularization

$$\dot{x}(t) = A\ x(t)\ +\ B\ w(t), \tag{11}$$

$$y(t) = C\ x(t)\ +\ D\ w(t). \tag{12}$$

The considered regularization method is more easily presented in the frequency domain. In this context, the estimation problem is to solve the equation

$$\tilde{Y}(s) = G_p(s)W(s) + N(s). \tag{13}$$

using the observations $\tilde{y}$ of the outputs y.

Assume we are able to compute the inverse transfer function $G_p^{-1}(s)$, a regularization method is constructed as follows. To suppress the high frequencies due to the measurement errors, the considered regularization (Tikhonov and Arsenin, 1977; Blum and Marquardt, 1997; Mhamdi and Marquardt, 1999) suggests the design of a parameter dependent family of functions $G_f(s, \alpha)$ operating on $\tilde{Y}$ according to

$$\hat{W}(s) = G_f(s, \alpha)\ G_p^{-1}(s)\tilde{Y}(s). \tag{14}$$

α is the regularization parameter (see Figure 1). $G_f(s, \alpha)$ is chosen such that $\hat{W}(s)$ approximates the true input $W(s)$ as good as possible despite non-vanishing noise $N(s)$. In particular, $G_f(s, \alpha)$ should be chosen such that

- $0 \leq G_f(s, \alpha) \leq 1,\ \forall\ \alpha, s$;
- $G_f(s, \alpha) \to 1$ non-decreasingly as $\alpha \to 0$ and $G_f(s, 0) = 1$;
- $\lim_{s \to \infty} G_f(s, \alpha) = 0,\ \forall \alpha > 0$, and $\lim_{\alpha \to \infty} G_f(s, \alpha) = 0$.

These conditions are sufficient for the time-domain operator T_α corresponding to $G_e(s) = G_f(s, \alpha)G_p^{-1}(s)$ to qualify as a regularization operator in the sense of equation (7) (Tikhonov and Arsenin, 1977).

These design specifications are in general conflicting, as seen from the expression of the estimation error $E_w(s) = \hat{W}(s) - W(s)$:

$$E_w(s) = (G_f(s, \alpha) - 1)\ W(s) + G_f(s, \alpha)\ G_p^{-1}(s)\ N(s). \tag{15}$$

The choice of an appropriate regularization parameter α is in general difficult. However, many

methods have been proposed in the literature for its computation (Engl *et al.*, 1996). Most of them are based on residual norms. They can be divided into two classes: (i) methods based on knowledge of the error level ϵ, e.g. Morozov's discrepancy principle; and (ii) methods that do not require the knowledge of ϵ, e.g. Generalized Cross Validation or the L-Curve Criterion (Hansen, 1998). The last method is used in this work.

Inversion of LTI systems has been considered in many publications. The approach developed by Silverman (Silverman, 1969) is most fruitful. The basic idea is to construct a sequence of systems system Σ_k

$$\dot{z}_k(t) = A_k\ z_k(t)\ +\ B_k\ w(t), \tag{16}$$
$$y_k(t) = C_k\ z_k(t)\ +\ D_k\ w(t), \tag{17}$$

by iteratively differentiating the output equation (12) until we reach an iteration $k = r$ where the corresponding matrix D_r is invertible.

Therefore D_r^{-1} exists, and we have after some algebraic manipulations the inverse system $\Sigma_L^\sharp$

$$\dot{z}(t) = (A - BD_r^{-1}C_r)\ z(t) + BD_r^{-1}y_r(t) \tag{18}$$
$$w(t) = -D_r^{-1}C_r z(t) + D_r^{-1}y_r(t) \tag{19}$$

with input vector y_r comprising time derivatives up to the order r of the system output y Hence, the obtained inverse system $\Sigma_L^\sharp$ is given by a cascade of the bank of differentiators to get y_r and the dynamical system given by (18)-(19).

A construction for the case $m \neq p$ has been given by Silverman and Payne (Silverman and Payne, 1971). The question of invertibility without knowledge of the initial states has been addressed by Moylan (1977).

4.2 Nonlinear systems

Consider now the nonlinear system (1)-(2) Σ_{NL}

$$\dot{x}(t) = A(x)\ +\ B(x)\ w(t),$$
$$y(t) = C(x)\ +D(x)\ w(t)$$

Since the the iterative procedure of Silverman for the construction of the inverse system is done in the time domain using differentiation and elementary algebraic operations, it has been already extended to time-varying and nonlinear systems (Hirschorn, 1979). A closed representation of the inverse system is (Daoutidis and Kravaris, 1991):

$$\dot{z} = A(z) - B(z)M^{-1}(z)\begin{bmatrix} L_f^{\beta_1}C_1(z) \\ \vdots \\ L_f^{\beta_p}C_p(z) \end{bmatrix} + B(z)M^{-1}(z)\begin{bmatrix} \frac{d^{\beta_1}y_1}{dt^{\beta_1}} \\ \vdots \\ \frac{d^{\beta_p}y_p}{dt^{\beta_p}} \end{bmatrix}, \tag{20}$$

$$w = B(z)M^{-1}(z)\left(\begin{bmatrix} L_f^{\beta_1}C_1(z) \\ \vdots \\ L_f^{\beta_p}C_p(z) \end{bmatrix} - \begin{bmatrix} \frac{d^{\beta_1}y_1}{dt^{\beta_1}} \\ \vdots \\ \frac{d^{\beta_p}y_p}{dt^{\beta_p}} \end{bmatrix}\right).$$

with

$$M(z) = \begin{bmatrix} L_{b_1}L_A^{\beta_1}c_1(z) & \cdots & L_{b_p}L_A^{\beta_1}c_1(z) \\ \vdots & & \vdots \\ L_{b_1}L_A^{\beta_p}c_p(z) & \cdots & L_{b_p}L_A^{\beta_p}c_p(z) \end{bmatrix}$$

As in the linear case, not only the system outputs, but also their derivatives are used as system inputs. This inverse is not suitable for input estimation without additional regularization, since unavoidable measurement errors lead to an error amplification in the solution.

The determination of the derivatives of the involved measured variable requires the solution of linear inverse problems. The method presented in the previous section is used here to solve them.

5. ILLUSTRATING EXAMPLE

The regularization procedure is illustrated by an example taken from (Farza *et al.*, 1998) using the same set of constant model parameters.

In a bioprocess, product P is made from biomass X and substrate S. The process modelling leads to the nonlinear system

$$\dot{X} = \mu X - DX, \tag{21}$$
$$\dot{P} = \nu X - DP, \tag{22}$$
$$\dot{S} = -\eta_1\mu X - \eta_2\nu X + D(S_{in} - S), \tag{23}$$

with initial conditions X_0, P_0 and S_0. where D is the dilution rate and η_1 and η_2 are yield coefficients. The quantities μ and ν define the specific reaction rates for the growth of the biomass and for the biosynthesis respectively, which are to be estimated from measurements of X and P. For the generation of the measured data in simulation the following models for μ and ν are used:

$$\mu = \mu_{max}\frac{S}{\left(K_{S_1} + S + \frac{S^2}{K_I}\right)}\frac{K_P}{(K_P + P)}\left(1 - \frac{P}{P_f}\right),$$
$$\nu = \nu_m ax\frac{S}{(K_{S_2} + S)}.$$

Figures 2-3 show the true and noisy measurements. The corresponding dilution rate D varies as a trapezoidal signal from 0.1 to $0.2/h$.

Instead of assuming kinetic models for μ and ν, these are regarded as unknown inputs w_1 and w_2 to a nonlinear dynamic system with the states $x_1 = X$ $x_2 = P$ and $x_3 = S$:

$$\dot{x}_1 = -Dx_1 + x_1 w_1 \tag{24}$$
$$\dot{x}_2 = -Dx_2 + x_1 w_2 \tag{25}$$
$$\dot{x}_3 = D(S_{in} - x_3) - \eta_1 x_1 w_1 - \eta_2 x_1 w_2. \tag{26}$$
$$y_1 = x_1 \tag{27}$$
$$y_2 = x_2 \tag{28}$$

The inverse system is then

$$\dot{z}_1 = \dot{y}_1 \tag{29}$$
$$\dot{z}_2 = \dot{y}_2 \tag{30}$$
$$w_1 = D + \frac{1}{z_1}\dot{y}_1 \tag{31}$$
$$w_2 = D\frac{z_2}{z_1} + \frac{1}{z_1}\dot{y}_2 \tag{32}$$

The results of the estimation are shown in Figures 4-7. Although the noise is relatively small, the calculated inputs are without regularization, as expected, not useful (Figures 4,5). A regularization with the approach described above results in reasonable estimates, as shown in Figures 6,7. The simulation was done with a second order transfer function G_f with a regularization parameter determined by the L-curve criterion.

6. CONCLUSIONS

We have considered, in this work, the estimation of unknown reaction rates based on the theory of inverse problems. The proposed estimator does not assume or require any model for the reaction rates. The method is based on system inversion and filtering. The design has been achieved for MIMO linear and nonlinear systems. The results obtained show that efficient and satisfactory estimations could be achieved.

As seen from our problem formulation, the method is not restricted to the estimation of reaction rates. It is applicable to problems where unknown inputs w are determined from measurements of other quantities using the considered model structure. Some other examples from chemical engineering are estimation of heat fluxes, heat of reaction or interphase mass transfer. Similar problems appear also in other engineering and science areas. Moreover, different types of system uncertainties such as nonlinearities, parameter changes, faults and unknown external excitation can be conveniently represented as unknown inputs. Therefore, the unknown input estimation method is of great interest for system supervision and robust or fault-tolerant control.

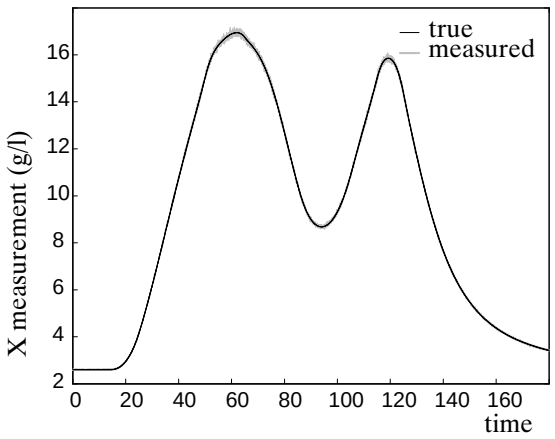

Fig. 2. Biomass concentration measurements

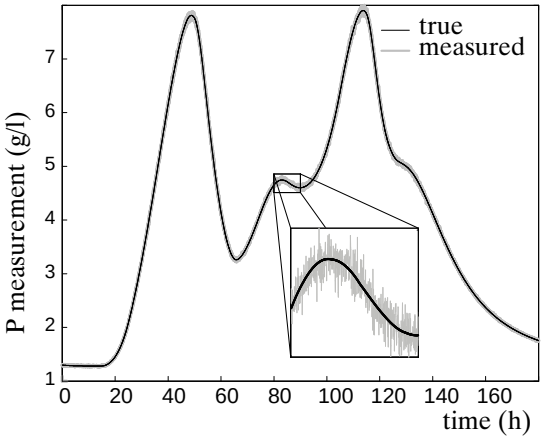

Fig. 3. Product concentration measurements

This work may be extended by considering other classes of systems where the inverse system may be determined.

ACKNOWLEDGMENTS

This work was funded by the Deutsche Forschungsgemeinschaft (DFG) within the Collaborative Research Center (SFB) 540 "Model-based Experimental Analysis of Kinetic Phenomena in Fluid Multi-phase Reactive Systems".

REFERENCES

Blum, J. and W. Marquardt (1997). An optimal solution to inverse heat conduction problems based on frequency domain interpretation and observers. *Numerical Heat Transfer, Part B:Fundamentals* **32**, 453–478.

Daoutidis, P. and C. Kravaris (1991). Inversion and zero dynamics in nonlinear multivariable control. *AIChE Journal* **37**(4), 527–538.

de Vallière, P. and D. Bonvin (1990). Application of estimation techniques to batch reactors - III: Modelling refinements which improve the quality of state and parameter esti-

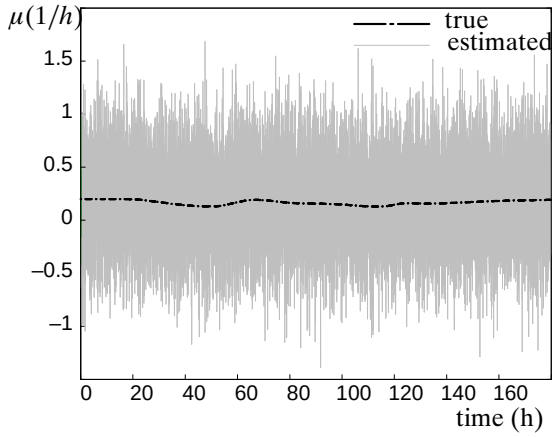

Fig. 4. True and estimated specific reaction rate μ without regularization

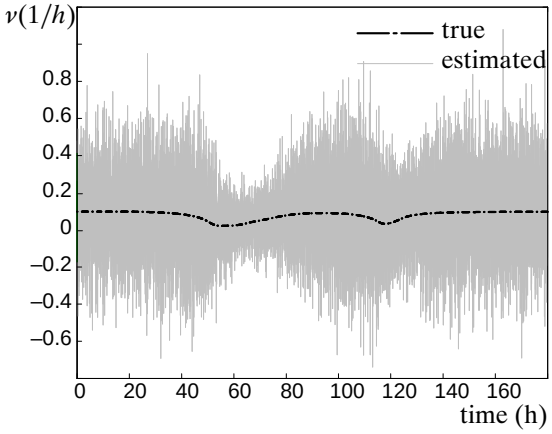

Fig. 5. True and estimated specific reaction rate ν without regularization

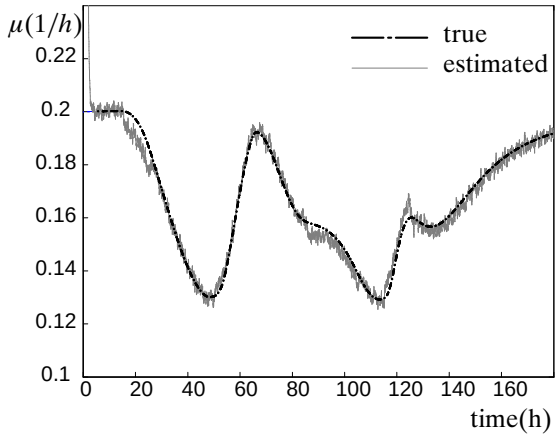

Fig. 6. True and estimated specific reaction rate μ with regularization

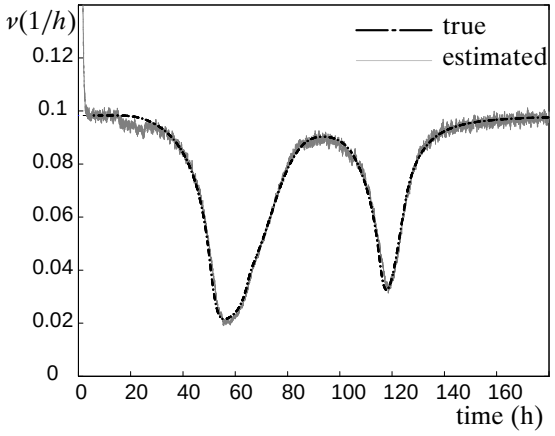

Fig. 7. True and estimated specific reaction rate ν with regularization

mation. *Computers and Chemical Engineering* **14**(7), 799–808.

Eliçabe, G. E., E. Ozdeger and C. Georgakis (1995). On-line estimation of reaction rates in semicontinuous reactors. *Ind. Eng. Chem. Res.* **34**, 1219–1227.

Engl, H. W., M. Hanke and A. Neubauer (1996). *Regularization of Inverse Problems*. Kluwer Academic Publishers.

Farza, M., K. Busawon and H. Hammouri (1998). Simple nonlinear observers for on-line estimation of kinetic rates in bioreactors. *Automatica* **34**(3), 312–318.

Hansen, C. (1998). *Rank-Deficient and Discrete Ill-posed Problems: Numerical Aspects of Linear Inversion*. SIAM Monographs on Mathematical Modeling and Computation. SIAM.

Hirschorn, R. M. (1979). Invertibility of nonlinear control systems. *SIAM J. Control and Optimization* **17**(2), 289–297.

Kirsch, A. (1996). *An Introduction to the Mathematical Theory of Inverse Problems*. Springer.

Mhamdi, A. and W. Marquardt (1999). An inversion approach to the estimation of reaction rate in chemical reactors. In: *Proc. European Control Conference ECC'99, Karlsruhe, Germany, 31.8.-3.9.*

Moylan, P. J. (1977). Stable inversion of linear systems. *IEEE Transactions on Automatic Control* **AC–22**(1), 74–78.

Schuler, H. and C. Schmidt (1992). Calorimetric state estimators for chemical reactor diagnosis and control: review of methods and applications. *Chemical Engineering Science* **47**, 899–915.

Silverman, L. and H.J. Payne (1971). Input-output structure of linear systems with application to the decoupling problem. *SIAM J. Control* **9**, 199–233.

Silverman, L. M. (1969). Inversion of multivariable linear systems. *IEEE Transactions on Automatic Control* **AC–14**(3), 270–276.

Tikhonov, A. N. and V. Y. Arsenin (1977). *Solutions of Ill-posed Problems*. V. H. Winston and Sons.

AN INCREMENTAL APPROACH FOR THE IDENTIFICATION OF REACTION KINETICS

Marc Brendel [*], **Adel Mhamdi** [*],
Dominique Bonvin [**], **Wolfgang Marquardt** [*,1]

[*] *Lehrstuhl für Prozesstechnik, RWTH Aachen University, D-52064 Aachen, Germany*
[**] *Laboratoire d'Automatique, EPFL, CH-1015 Lausanne, Switzerland*

Abstract: This paper proposes an incremental approach for the identification of complex reaction kinetics in chemical reactors. The reaction fluxes for the various species are first estimated on the basis of concentration measurements and balance equations. This task represents an ill-posed inverse problem requiring appropriate regularization. In a further step, the reaction rates are estimated without postulating a kinetic structure. Finally, the dependency of the reaction rates on concentrations, i.e. the kinetic laws, are constructed by means of feed-forward neural networks. This incremental approach is shown to be both efficient and flexible for utilizing the available process knowledge. The methodology is illustrated on the industrially-relevant acetoacetylation of pyrrole with diketene.

Keywords: Identification, reactor modeling, input estimation, regularization, neural networks

1. INTRODUCTION

The description of reaction kinetics often represents the most challenging part in the modeling of chemical reactors. A reliable description is rarely available a priori. For example, it is well known that reaction kinetics cannot necessarily be derived from stoichiometries (Connors, 1990), in particular in the case of catalyzed reactions. Thus, a reliable kinetic model needs to be identified from experimental data.

The model-based techniques used in process control and optimization require a model that adequately describes the process dynamics, i.e. also the kinetics in reaction systems. For the case where a kinetic structure is not available, Psichogios and Ungar (1992) proposed a hybrid approach to process modeling as an alternative to recurrent neural networks for describing the dynamic system. The hybrid model combines prior knowledge on mass and energy balances with a feed-forward neural net model that serves as a substitute for the constitutive equations that cannot be determined from first principles. These authors found that the hybrid model has better properties than standard black-box neural net models, i.e. interpolation and extrapolation are more accurate and the model is easier to analyze and interpret. Parameters in the neural net part of the hybrid model can be estimated from experimental data. Recently, Tholudur and Ramirez (1999) used a two-step approach for the identification of kinetics: Reaction rates are first identified, assuming known curve characteristics, and subsequently correlated with the independent state variables using a feed-forward neural net approximation. Van Lith *et al.* (2002) combined

[1] Corresponding author. E-mail: marquardt@lfpt.rwth-aachen.de

an extended Kalman filter for the estimation of states and rates with subsequent fuzzy submodel identification.

In this work, an incremental approach for the identification of reaction kinetics is proposed when no prior kinetic knowledge is available. The approach is applicable to all reactor types, i.e. also to those exhibiting transient behavior and possibly variable feed and effluent streams. The reaction fluxes for the various species are estimated from noisy concentration data using the approach of Mhamdi and Marquardt (1999). Then, the individual reaction rates can be calculated using knowledge of reaction stoichiometry. These reaction rates and the concentration data serve as input to a Bayesian algorithm to train a feed-forward neural network yielding the kinetic model. The approach is especially suited for nowaday's high resolution measurement techniques such as IR (Alsmeyer *et al.*, 2002) or Raman spectroscopy (Bardow *et al.*, 2003), where concentration data can be obtained continuously in-situ.

2. PRELIMINARIES

2.1 Model of the reaction system

Consider a homogeneous, not necessarily isothermal, chemical reaction system with R reactions involving S species. The time evolution of the number of moles of species i, n_i [mol], is given by:

$$\frac{\mathrm{d}n_i}{\mathrm{d}t} = f_i^{\mathrm{in}} - f_i^{\mathrm{out}} + f_i^{\mathrm{r}} \ , \quad i = 1, .., S \tag{1}$$

where f_i^{in} and f_i^{out} [mol/min] are the molar flow rates of species i into and out of the reactor and f_i^{r} [mol/min] is the reaction flux of species i, i.e. the net molar flow rate of species i produced or consumed by the various chemical reactions.

The reaction flux of species i can be expressed in terms of the individual reaction rates:

$$f_i^{\mathrm{r}} = V \sum_j^R \nu_{ij} r_j, \quad i = 1, .., S \tag{2}$$

where ν_{ij} is the stoichiometric coefficient for species i in the jth reaction, r_j [mol/l min] the rate of the jth reaction, and V [l] the volume.

In vector form, equation (2) reads:

$$\mathbf{f}^{\mathrm{r}} = V\mathbf{N}\mathbf{r} \tag{3}$$

where $\mathbf{f}^{\mathrm{r}}$ is the S-dimensional reaction flux vector, $\mathbf{r}$ the R-dimensional reaction rate vector and $\mathbf{N}$ the $S \times R$ stoichiometric matrix.

Equation (3) indicates that, if $S \geq R$, the reaction rate vector can be calculated from the reaction fluxes as follows:

$$\mathbf{r} = \frac{1}{V}\mathbf{N}^{+}\mathbf{f}^{\mathrm{r}} \tag{4}$$

where $\mathbf{N}^{+}$ is the Moore-Penrose inverse of $\mathbf{N}$.

For a constant-density semi-batch reactor with a volumetric feed of rate F [l/min] and concentration c_i^{in} [mol/l] and no outflow, the mole balance equation (1) expressed in terms of the molar concentration $c_i = n_i/V$ [mol/l], and the total mass balance give

$$\frac{\mathrm{d}c_i}{\mathrm{d}t} = \frac{F}{V}(c_i^{\mathrm{in}} - c_i) + \frac{f_i^{\mathrm{r}}}{V} \tag{5}$$

$$\frac{\mathrm{d}V}{\mathrm{d}t} = F, \tag{6}$$

implying no volume change by the reactions.

2.2 Estimation of reaction fluxes

The reaction fluxes $f_i^{\mathrm{r}}(t)$ can be estimated independently for each species. A generic model of the problem is developed as follows. Let

$$y_i(t) = n_i(t) - n_i(t_0) - \int_{t_0}^{t} u_i(\tau)\ d\tau, \tag{7}$$

where $u_i(\tau) = f_i^{\mathrm{in}}(\tau) - f_i^{\mathrm{out}}(\tau)$. This transformation, applied to (1), leads to

$$\frac{\mathrm{d}y_i(t)}{\mathrm{d}t} = f_i^{\mathrm{r}}(t),\ y_i(t_0) = 0, \tag{8}$$

where $f_i^{\mathrm{r}}(t)$ is considered as an unknown input that must be determined on the basis of a noisy measurement

$$\tilde{y}_i(t) = y_i(t) + \varepsilon_{y_i}(t). \tag{9}$$

Here, the superscript $(\tilde{\cdot})$ is used to denote a noisy quantity and ε_y represents the measurement noise contained in $\tilde{y}$.

This estimation problem represents an ill-posed inverse problem according to the definition of Hadamard (Engl *et al.*, 1996). Since the measurement is noisy, the estimate $\hat{f}_i^{\mathrm{r}}(t)$ of $f_i^{\mathrm{r}}(t)$ can be arbitrarily large if no regularization of the solution is considered. Mhamdi and Marquardt (1999) used Tikhonov-Arsenin filtering for the estimation of $f_i^{\mathrm{r}}(t)$. The quality of the estimation is greatly influenced by the choice of the regularization parameter that weighs the tradeoff between noise reduction and bias in the estimate. Adequate regularization parameters can be determined by the *L-curve criterion* (Hansen, 1998), for example.

Another approach to filtering is the use of smoothing splines (Craven and Wahba, 1979). Splines are piecewise polynomial functions that possess certain smoothness and differentiability properties at the nodes. *General cross validation (GCV)* is often used to select a suitable regularization parameter (Craven and Wahba, 1979).

3. INCREMENTAL IDENTIFICATION APPROACH

The incremental identification approach mirrors the steps taken when developing a model for a given process. During model development, the balance equations are set up first and the unknown fluxes are then described by constitutive equations. If needed, variable parameters in the constitutive equations can be modeled as functions of the system states. Transferring this procedure to the identification process, the incremental identification approach features the stepwise identification of quantities as they are used in the modeling process. In an adaptive model identification context (Marquardt, 2002), the incremental approach allows the utilization of as much information as can be safely provided by first-principle modeling or sound empirical approaches. The process of identification then reduces to modeling uncertainties, i.e. unknown parameters in a given structure or the model structure itself. This way, the identification procedure is split up into a sequence of decoupled identification problems. This offers two main advantages: i) the solution at a given step becomes more simple as e.g. process dynamics are considered in the first step and can be omitted subsequently, and ii) physical insight is provided for tackling the following steps.

The incremental identification approach for the identification of reaction kinetics is depicted in Figure 1. It includes the following steps:

(1) The fluxes $\hat{f}_i^{\mathrm{r}}(t)$, i=1, .., S are estimated using mole balances (Model 1). Use equations (7)-(9) and $\tilde{n}_i = \tilde{c}_i V$.
(2) With additional information on stoichiometry (Model 2), the reaction rates $\hat{r}_j(t)$, j=1, .., R are then calculated using (4).
(3) Furthermore, if the rate laws (e.g. $r = kc_A c_B$) are known (Model 3), (time-variant) rate constants $\hat{k}_j(t)$ are calculated from the reaction rate $\hat{r}_j(t)$ and concentrations $\hat{c}_i(t)$.
(4) Model 4 in addition assumes a temperature dependency of k such as the Arrhenius law ($k = k_0 e^{\frac{-E}{RT}}$). The rate constant parameters ($\hat{k}_{0j}$, $\hat{E}_j$) can then be estimated from $\hat{k}_j(t)$ and $\hat{T}(t)$.

If parts of the kinetics are unknown, such as the Arrhenius law, the outputs of Model 3 can be taken as inputs to a data-driven approach for describing $k = k(T)$. For an unknown rate law (Model 2 known), $\hat{c}_i$, T and $\hat{r}_j$ serve as inputs to the data-driven models $r_j = r_j(c_i)$ and $r_j = r_j(c_i, T)$ for the isothermal and non-isothermal cases, respectively. If the reaction stoichiometry is unknown, target factor analysis (Bonvin and Rippin, 1990) can help identify the stoichiometry based on the estimated fluxes.

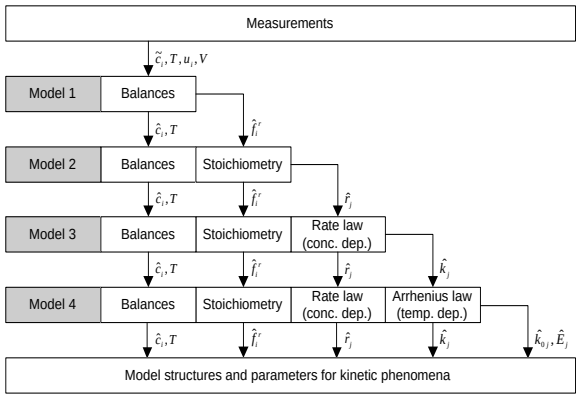

Fig. 1. Incremental approach for reaction kinetics identification

For describing functional relations in a data set, methods can be grouped in two categories based on the quality and amount of prior knowledge. If a model structure is available, the unknown model parameters can be identified from the data. Lacking such a model structure, black-box approaches are usually used, with the choice of basis functions based on some prior knowledge. Their ability to approximate any function arbitrarily well, given a sufficient number of parameters, may imply overfitting where the error on the training set is small, but a large error results if new data are presented to the model. To avoid overfitting and improve the predictive capability of the model, regularization, model discrimination or data validation techniques are commonly used. Feed-forward neural networks with Bayesian regularization (MacKay, 1992) may serve as an automated regularization procedure for training.

4. ILLUSTRATIVE EXAMPLE

4.1 Simulated reaction system

The incremental approach for identifying reaction kinetics is illustrated on the acetoacetylation of pyrrole with diketene (Ruppen *et al.*, 1997):

$$\mathrm{P{+}D} \xrightarrow{\mathrm{K}} \mathrm{PAA} \tag{10a}$$

$$\mathrm{D{+}D} \xrightarrow{\mathrm{K}} \mathrm{DHA} \tag{10b}$$

$$\mathrm{D} \rightarrow \text{oligomers} \tag{10c}$$

$$\mathrm{PAA{+}D} \xrightarrow{\mathrm{K}} \mathrm{F} \tag{10d}$$

In addition to the desired reaction of diketene (D) and pyrrole (P) to 2-acetoacetyl pyrrole (PAA) (10a), there are several undesired side reactions (10b)-(10d). These include the dimerization and oligomerization of diketene to dehydroacetic acid (DHA) and oligomers as well as a consecutive reaction to the by-product F. The reactions take place isothermally in a laboratory-scale semi-batch reactor with an initial volume of 1 liter, to which a diluted solution of diketene is added continuously.

Reactions (10a), (10b) and (10d) are catalyzed by pyridine (K), the concentration of which continuously decreases during the run due to addition of the diluted diketene feed. The dilution of catalyst is modeled by normalizing the corresponding rate constants with respect to the volume. Reaction (10c), which is assumed to be promoted by other intermediate products, is not normalized. Hence, the effective reaction rates are described by the following constitutive equations

$$r_j(t) = \frac{V_0}{V(t)} r_j^\star(t), \quad j = \{a, b, d\}, \tag{11}$$

$$r_c(t) = r_c^\star(t), \tag{12}$$

with the formal reaction rates

$$r_a^\star(t) = k_a c_{\mathrm{P}}(t) c_{\mathrm{D}}(t), \tag{13a}$$

$$r_b^\star(t) = k_b c_{\mathrm{D}}^2(t), \tag{13b}$$

$$r_c^\star(t) = k_c c_{\mathrm{D}}(t), \tag{13c}$$

$$r_d^\star(t) = k_d c_{\mathrm{PAA}}(t) c_{\mathrm{D}}(t), \tag{13d}$$

where k_a, k_b, k_c and k_d represent the rate constants and V_0 the initial volume.

The mole balances for the species D, P, PAA and DHA read

$$\frac{\mathrm{d}c_{\mathrm{D}}(t)}{\mathrm{d}t} = \frac{F(t)}{V(t)}[c_{\mathrm{D}}^{\mathrm{in}} - c_{\mathrm{D}}(t)] + \frac{f_{\mathrm{D}}^{\mathrm{r}}(t)}{V(t)}, \tag{14a}$$

$$\frac{\mathrm{d}c_{\mathrm{P}}(t)}{\mathrm{d}t} = -\frac{F(t)}{V(t)} c_{\mathrm{P}}(t) + \frac{f_{\mathrm{P}}^{\mathrm{r}}(t)}{V(t)}, \tag{14b}$$

$$\frac{\mathrm{d}c_{\mathrm{PAA}}(t)}{\mathrm{d}t} = -\frac{F(t)}{V(t)} c_{\mathrm{PAA}}(t) + \frac{f_{\mathrm{PAA}}^{\mathrm{r}}(t)}{V(t)}, \tag{14c}$$

$$\frac{\mathrm{d}c_{\mathrm{DHA}}(t)}{\mathrm{d}t} = -\frac{F(t)}{V(t)} c_{\mathrm{DHA}}(t) + \frac{f_{\mathrm{DHA}}^{\mathrm{r}}(t)}{V(t)}, \tag{14d}$$

with the initial conditions $c_{\mathrm{D}}(0) = c_{\mathrm{D0}}$, $c_{\mathrm{P}}(0) = c_{\mathrm{P0}}$, $c_{\mathrm{PAA}}(0) = c_{\mathrm{PAA0}}$ and $c_{\mathrm{DHA}}(0) = c_{\mathrm{DHA0}}$. The reaction fluxes $f_{\mathrm{D}}^{\mathrm{r}}$, $f_{\mathrm{P}}^{\mathrm{r}}$, $f_{\mathrm{PAA}}^{\mathrm{r}}$ and $f_{\mathrm{DHA}}^{\mathrm{r}}$ can be related to the reaction rates using the stoichiometry:

$$f_{\mathrm{D}}^{\mathrm{r}} = (-r_a - 2r_b - r_c - r_d)V, \tag{15a}$$

$$f_{\mathrm{P}}^{\mathrm{r}} = -r_a V, \tag{15b}$$

$$f_{\mathrm{PAA}}^{\mathrm{r}} = (r_a - r_d)V, \tag{15c}$$

$$f_{\mathrm{DHA}}^{\mathrm{r}} = r_b V. \tag{15d}$$

4.2 Experimental design

To assess the capability of the incremental identification approach and allow a comparison of the modeled and true kinetics, concentration trajectories are generated using the model described above and the rate constants given in Table 1.

The measured concentrations are assumed to stem from a high-resolution in-situ measurement technique such as Raman spectroscopy, taken at a sampling frequency $f_{\mathrm{s}} = 60$ min^{-1} and corrupted with normally distributed white noise of standard deviation $\sigma_{\mathrm{c}} = 0.01$ mol/l. The batch time is $t_{\mathrm{f}} = 60$ min. Concentration data are available for the species D, P, PAA and DHA, but not for the oligomers and the side product F since the latter are difficult to obtain.

Table 1. Values of rate constants

	k_a $[\frac{l}{molmin}]$	k_b $[\frac{l}{molmin}]$	k_c $[\frac{1}{min}]$	k_d $[\frac{l}{molmin}]$
value	0.053	0.128	0.028	0.001

Table 2. Range of independent variables

	c_{D0} $[\frac{mol}{l}]$	c_{P0} $[\frac{mol}{l}]$	c_{PAA0} $[\frac{mol}{l}]$	c_{DHA0} $[\frac{mol}{l}]$	F $[\frac{l}{min}]$	$c_{\mathrm{D}}^{\mathrm{in}}$ $[\frac{mol}{l}]$
min	0.07	0.40	0.10	0.02	0.5e-3	4.0
max	0.14	0.80	0.20	0.04	1.5e-3	6.0

The reaction system (10a)-(10d) suggests that r_b and r_c are univariate functions of c_{D}, whereas r_a and r_d are expected to be bivariate functions of c_{P}, c_{D} and c_{PAA}, c_{D}, respectively.

To obtain reliable approximations of the reaction rates, in particular for the bivariate functions, experiments are designed so as to obtain concentration data over a large domain. Six independent variables can be considered: the four initial conditions c_{D0}, c_{P0}, c_{PAA0} and c_{DHA0}, feed rate F chosen to be constant during a run, and feed concentration $c_{\mathrm{D}}^{\mathrm{in}}$. The possible ranges of these independent variables are given in Table 2. Since c_{D0}, c_{P0}, F and $c_{\mathrm{D}}^{\mathrm{in}}$ have the largest impact on the resulting transient behavior, a 2^{6-2} factorial design consisting of 16 experiments is selected. Fewer experimental runs would reduce the validity range and/or the predictive capability of the model, while additional runs would improve them.

4.3 Various modeling scenarios

In the following, three different modeling scenarios are presented, each differing in the amount of prior knowledge regarding the reactions. The fluxes, reaction rates and reaction kinetics are identified from noisy concentration measurements.

Scenario 1 In the first scenario, we assume knowledge regarding the existence of reactions (10a)-(10d), including their stoichiometric coefficients. Moreover, it is known that the rates of the reactions (10a), (10b) and (10d) are proportional to the catalyst concentration, see (11).

The reaction fluxes for the various species are obtained from (8) using appropriate regularization. Here, smoothing splines with GCV are used for determining the regularization parameters.

From the time-dependent reaction fluxes f_i^{r}, $i = \{\mathrm{D}, \mathrm{P}, \mathrm{PAA}, \mathrm{DHA}\}$, the time-dependent reaction

rates r_j, $j = \{a, b, c, d\}$, can be calculated using (15a)-(15d). Since the influence of the catalyst on the reaction rates is known, the formal reaction rates $r_j^\star$ are determined from (11) and (12).

Finally, the concentrations and the reaction rates from one or several runs are correlated as $r_a^\star = r_a^\star(c_\mathrm{P}, c_\mathrm{D})$, $r_b^\star = r_b^\star(c_\mathrm{D})$, $r_c^\star = r_c^\star(c_\mathrm{D})$ and $r_d^\star = r_d^\star(c_\mathrm{PAA}, c_\mathrm{D})$, as proposed by stoichiometry. A feed-forward neural net with Bayesian regularization as training algorithm and 3 nodes in the hidden layer is utilized.

Scenario 2 In the second scenario, no information regarding the effect of catalyst on the kinetics is postulated. This corresponds to $r_j^\star = r_j$. Otherwise, the procedure is identical to that of Scenario 1.

Scenario 3 We consider the case where little is known a priori about the reaction system. Besides the known desired reaction (10a), there is evidence that diketene (D) and pyrrole (P) are involved in other reactions, including the formation of the dimerization product DHA. Hence, the stoichiometric model

$$\mathrm{P{+}D} \rightarrow \mathrm{PAA} \tag{16a}$$

$$\mathrm{D} + \nu_1\mathrm{PAA} \rightarrow \nu_2\mathrm{DHA} + \mathrm{G} \tag{16b}$$

is postulated, where the possible side reactions are lumped into reaction (16b) with the unknown stoichiometric coefficients ν_1 and ν_2 and some unknown side products G.

From the estimated reaction fluxes, the reaction rates $r_a^\star(\mathrm{t})$ for Reaction (16a) and $r_\mathrm{lump}^\star(\mathrm{t})$ for Reaction (16b) as well as the stoichiometric coefficients ν_1 and ν_2 can be determined as solution of the reconciliation problem:

$$f_\mathrm{D}^\mathrm{r}(t) = [-r_a^\star(t) - r_{lump}^\star(t)]V(t) \tag{17a}$$

$$f_\mathrm{P}^\mathrm{r}(t) = -r_a^\star(t)V(t) \tag{17b}$$

$$f_\mathrm{PAA}^\mathrm{r}(t) = [r_a^\star(t) - \nu_1 r_{lump}^\star(t)]V(t) \tag{17c}$$

$$f_\mathrm{DHA}^\mathrm{r}(t) = \nu_2 r_{lump}^\star(t)V(t). \tag{17d}$$

The rates $r_a^\star(\mathrm{t})$ and $r_\mathrm{lump}^\star(\mathrm{t})$ can subsequently be correlated with the concentrations, as discussed in Scenario 1.

4.4 Identification results

Reaction fluxes and concentrations Exemplarily, the true and estimated reaction fluxes for species D are shown in Figure 2 (right). Integration of (14a) yields an estimate of the concentration c_D, as shown in Figure 2 (left).

Reaction rates For Scenario 1, the estimated rate $r_b^\star$ in the univariate case is shown in Figure 3, along with training data and true rate.

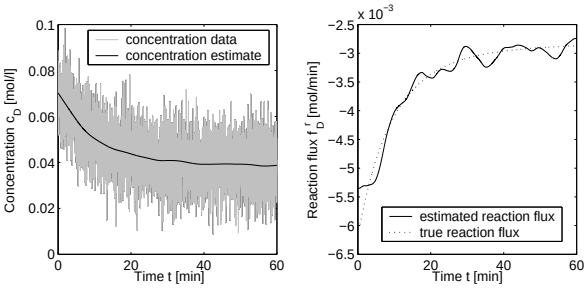

Fig. 2. True and estimated reaction flux f_D^r (right), measured and estimated concentration c_D (left)

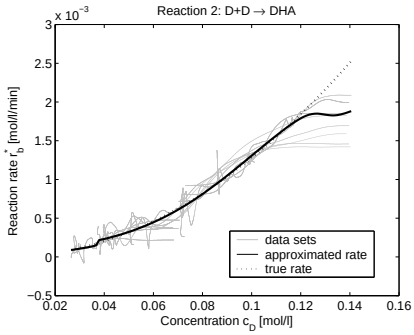

Fig. 3. Estimated reaction rate $r_b^\star$

Kinetic model The validity range of a model is defined as the smallest n-dimensional (e.g. $n = 2$ for the bivariate case) box containing all concentration combinations taken for training. The mean and maximum values of the neural net predictions in the validity range are compared to the true (simulated) reaction rates in Table 3.

The predictions obtained in Scenarios 2 and 3 are comparable which can be accredited to the fact that the volume change remains small during the runs (the increase in volume does not exceed 3% for the low and 9% for the high feed rate). Presumably, the importance of the catalyst dilution becomes more obvious for large volume changes. Rate $r_d^\star$, whose value is small compared to the other rates, is mainly influenced by noise and cannot be identified satisfactorily.

For the lumped model in Scenario 3, the main reaction rate $r_a^\star$ is identified with reasonable accuracy despite the error introduced by lumping all side reactions in (16b). Here, the stoichiometric coefficients ν_1 and ν_2 were calculated as 0.0028 and 0.2227, respectively. Since the rates $r_b^\star$, $r_c^\star$ and $r_d^\star$ were not modeled, they are not identified in this case.

Table 3. Reaction rate prediction errors

		$r_a^\star$	$r_b^\star$	$r_c^\star$	$r_d^\star$
Scenario 1	Mean error	2.95	6.15	5.16	185
	Max. error	11.24	26.42	20.92	3245
Scenario 2	Mean error	4.48	7.33	4.88	117
	Max. error	15.69	25.84	18.58	466
Scenario 3	Mean error	4.64	-	-	-
	Max. error	62.99	-	-	-

4.5 Validation of the hybrid model

To check the predictive capability of the hybrid model consisting of the mole balance equations and the neural-net-based kinetic laws, concentration trajectories are simulated using (13a)-(13d) and the neural net approximations used to predict them. Ten runs were simulated with experimental conditions chosen randomly within the ranges given in Table 2. The mean and maximum values of the prediction errors are listed in Table 4.

Table 4. Hybrid model prediction errors

	[%]	c_{D}	c_{P}	c_{PAA}	c_{DHA}
Scenario 1	Mean error	0.81	0.11	0.40	1.10
	Max. error	2.80	0.63	1.48	5.58
Scenario 2	Mean error	0.79	0.24	0.61	1.10
	Max. error	2.30	0.43	1.19	5.04
Scenario 3	Mean error	0.60	0.20	0.53	4.13
	Max. error	1.91	0.42	1.28	15.58

Hybrid model predictions show excellent agreement with the true (simulated) values. The fact that the model predictions are good even for a poorly estimated reaction rate $r_d^\star$ illustrates the difficulties experienced in estimating this rate. These results suggest omitting reaction (10d) in the postulated reaction scheme. Comparison of the three scenarios also indicates that the hybrid model derived from the lumped model equations performs nearly as well as the detailed models.

5. CONCLUSIONS

This work has proposed an incremental approach for the identification of unknown kinetics in a chemical reactor. The approach consists of: (i) model-free estimation of the reaction flux associated with each species, (ii) calculation of the reaction rates using the (partially) known system stoichiometry, and (iii) identification of kinetic models using neural nets to represent the correlation between reaction rates and concentrations. Here, information on stoichiometry helps choosing the independent variables.

The predictive capability of the hybrid model was very satisfying as were the kinetics identified in the case of known stoichiometry. The errors observed were largely caused by missing initial information regarding the reaction fluxes, a phenomenon that requires further investigation.

It should be emphasized that the proposed incremental modeling approach is by no means limited to the use of neural net submodels. Mechanistic models using target factor analysis, multidimensional sparse grids or multigrid methods may also take advantage of the incremental approach.

ACKNOWLEDGEMENTS

This work was partially funded by the Deutsche Forschungsgemeinschaft (DFG) within the Collaborative Research Center (SFB 540) "Model-based experimental analysis of kinetic phenomena in fluid multiphase reactive systems"

REFERENCES

Alsmeyer, F., W. Marquardt and G. Olf (2002). A new method for phase equilibrium measurements in reacting mixtures. *Fluid Phase Equilibria* **203**, 31–51.

Bardow, A., W. Marquardt, V. Goeke, H.-J. Koss and K. Lucas (2003). Model-based measurement of diffusion using Raman spectroscopy. *AIChE Journal* **49**(2), 323–334.

Bonvin, D. and D. W. T. Rippin (1990). Target factor analysis for the identification of stoichiometric models. *Chemical Engineering Science* **45**(12), 3417–3426.

Connors, K. A. (1990). *Chemical Kinetics: The Study of Reaction Rates in Solution*. VCH publishers. New York.

Craven, P. and G. Wahba (1979). Smoothing noisy data with spline functions. *Numer. Math.* **31**, 377–403.

Engl, H. W., M. Hanke and A. Neubauer (1996). *Regularization of Inverse Problems*. Kluwer Academic Publishers. Dordrecht.

Hansen, P. C. (1998). *Rank-deficient and Discrete Ill-posed Problems*. SIAM. Philadelphia.

MacKay, D. J. C. (1992). Bayesian interpolation. *Neural computation* **4**(3), 415–447.

Marquardt, W. (2002). Adaptivity in process systems modeling. In: *Proc. European Symposium on Computer Aided Process Engineering (ESCAPE-12)*. Elsevier. The Hague, The Netherlands. pp. 42–56.

Mhamdi, A. and W. Marquardt (1999). An inversion approach to the estimation of reaction rates in chemical reactors. In: *Proc. European Control Conference (ECC'99)*. Karlsruhe, Germany. Paper F1004-1.

Psichogios, D. C. and L. H. Ungar (1992). A hybrid neural network - first principles approach to process modeling. *AIChE Journal* **38**(10), 1499–1511.

Ruppen, D., D. Bonvin and D. W. T. Rippin (1997). Implementation of adaptive optimal operation for a semi-batch reaction system. *Computers Chem. Engng.* **22**(1–2), 185–199.

Tholudur, A. and W. F. Ramirez (1999). Neural-network modeling and optimization of induced foreign protein production. *AIChE Journal* **45**(8), 1660–1670.

Van Lith, P. F., B. H. L. Betlem and B. Roffel (2002). A structured modeling approach for dynamic hybrid fuzzy first-principles models. *J. Proc. Cont.* **12**, 605–615.